Universidad de Concepción
Facultad de Ciencias Físicas y Matemáticas
Departamento de Ingeniería Matemática

A conservative HDG method for a coupled Navier-Stokes and Advection-Diffusion equation

por

Estefanía Belén Olivares Zamora

Tesis presentada a la Facultad de Ciencias Físicas y Matemáticas de la Universidad de Concepción para optar al título profesional de Ingeniera Civil Matemática

Profesores Guías: Manuel Solano (Universidad de Concepción)
Sander Rhebergen (University of Waterloo).

August 5, 2025,
Concepción, Chile.

EVALUATION COMMITTEE

Dr. Manuel Solano [Profesor guía]

Departamento de Ingeniería Matemática, Universidad de Concepción, Chile.

Dr. Sander Rhebergen

Deparment of applied math, Universidad de Waterloo, Canadá.

Dr. Rommel Bustinza

Departamento de Ingeniería Matemática, Universidad de Concepción, Chile.

Dr. Ricardo Oyarzúa

Departamento de Matemática, Universidad del Bio Bio, Chile.

DEFENSE: 22 August 2025.

Acknowledgments

A mi madre, Cecilia, que me apoyó desde el momento cero en que inicié esta carrera —y mucho antes aún—, me dio la fuerza y el ánimo para seguir cada año que pasaba, y en este último proceso de cierre no sé qué habría hecho sin ella. Gracias por las videollamadas diarias, que me hacían sentir un poco más cerca de ti, a pesar de estar a más de dos mil kilómetros. Eres mi modelo a seguir, y realmente espero, algún día, ser la mitad de la gran mujer que eres tú, mamá.

A mi padre, Luis, que siempre tuvo el consejo adecuado y sabio en este camino. Gracias por todas esas llamadas que realizamos mientras caminaba a la universidad o de vuelta. Estoy agradecida de que, aunque estuviéramos lejos, me sentí más cerca que nunca contigo durante estos años. Gracias por siempre estar, aunque sea a tu manera.

A mis hermanos, que sin ellos nada de esto sería posible, y que, cada uno a su manera, me apoyó y me dio ánimos para no desistir. A Luis —o más bien, Lucho para mí—, gracias por, a pesar de ser de pocas palabras, siempre tener esa preocupación hacia mí. Gracias por todos esos años de infancia en los que creamos bonitos recuerdos y, sobre todo, gracias por (a tu manera) ser un rol paternal hacia mí. A Alejandra, que las palabras no me alcanzan para agradecer todo lo que has hecho por mí en mis años de vida: mi segunda madre, mi confidente y mi mejor amiga. Gracias por hacerme parte de tu vida y, a pesar de que no siempre coincidamos en opinión, eres mi rol a seguir cada día. A Emanuel, que, a medida que vamos creciendo, nos vamos acercando más y entendiendo mejor. Gracias por siempre presentarme un juego nuevo con el cual distraerme. Gracias porque, ahora que estamos lejos, los momentos juntos los disfrutamos más que nunca, y, sobre todo, gracias por siempre hacer que nos riamos a carcajadas con chistes que solo nosotros entendemos.

A mis sobrinos, que son la luz de mis ojos. A Isaías, que más que un sobrino es mi hermano chico, gracias por la compañía (literal) estos años. Hemos estado toda la vida acompañándonos y espero que siga así por muchos años más. A Araceli y Samantha, o como yo les digo siempre, Jazmín y Denisse, las niñas de mis ojos. Todo lo que pase de aquí en adelante lo hago pensando en ustedes. Gracias por todas las videollamadas, incluso las en silencio, en las que solo nos acompañamos.

A Fernando y Luciano, que estuvimos juntos durante esta etapa. Gracias por todas las risas, los llantos, las desveladas, las paniqueadas y, sobre todo, las comidas. Gracias por su amistad todos estos años. Espero que, ahora que tomamos distintos caminos, sigamos contando el uno con el otro. Agradezco el día en que decidimos tomar ese electivo que, a pesar de lo peculiar que fue, me entregó a mis mejores amigos.

A Ricardo, Bastián, Patricio y Catalina, que, a pesar de no hablar tan seguido ni vernos tanto, me han enseñado el valor de la amistad.

A David, con quien he compartido tantas emociones y momentos. Gracias por estos años compartiendo vida. Gracias por permitirme crecer a tu lado y porque ambos hemos aprendido en el proceso. Por ello, estaré eternamente agradecida.

A mi Rukia, que no puedo describir lo agradecida que estoy por haberme dado 15 años siendo compañeras de vida, y por darme a mi Bobby. Te extrañamos un montón.

Esperando que no se me escape nadie en estos agradecimientos, doy gracias a todas las personas que fueron parte de mi vida universitaria, tanto dentro como fuera de la universidad. Gracias a todos los profesores que me topé durante el camino, que, más que un ramo, nos enseñaban sobre la vida.

También agradecer a los profesores Sander, Rommel y Ricardo por aceptar ser parte de mi comisión evaluadora. Gracias al profesor Manuel por aceptarme como su estudiante tesista hace poco más de un año. Espero haber estado a la altura.

Finalmente, gracias a los proyectos ANILLO ACT210087 y FONDECYT N° 1240183 por el financiamiento entregado para la realización de esta investigación.

Contents

Agradecimientos **iv**

Contents **vi**

List of figures **viii**

Resumen **ix**

1 Introduction **1**

1.1 Preliminaries 4

2 The advection-diffusion equations **7**

2.1 An HDG scheme for the Advection-Diffusion Equation equation. 8

2.2 Well-posedness. 11

3 The Navier-Stokes equations **17**

3.1 An HDG scheme for the Navier-Stokes equations. 18

3.1.1 Derivation of the discrete momentum equation. 18

3.1.2 Derivation of the discrete mass equation. 20

3.2 Well-posedness. 22

4 The Coupled Problem. 27

5 Error analysis. 34

6 Numerical simulations 41

6.1 Manufactured solutions. 42

6.1.1 Simulations in a desalination channel. 47

7 Conclusions and future work 51

7.1 Conclusions. 51

7.2 Future work. 52

Bibliography 55

List of Figures

1.1 Depicting of a single desalination channel. 2

6.1 Example 1. Domain $\Omega := (0, 1) \times (0, 1)$. 43

6.2 Concentration with $h = 0.0125$ and $k = 2$. Example 1. 44

6.3 Example 2. $\Omega = (0.1, 0.4) \times (0.0, 0.4)$. 45

6.4 Concentration with $h = 0.0125$ and order $k = 3$ 46

6.5 Comparison of exact vs. approximate pressure drop (bottom) and axial velocity (top) for a single channel. Simulation conditions: $u_{\text{in}} = 0.2\ m/s$, $\Delta P = \Delta P_2$ and clean water, $h = 4, 8e - 4$ and $k = 2$ 48

6.6 Concentration profile at the membrane. Simulation conditions: $u_{in} = 0.1m/s$, $\Delta P = \Delta P1$ 49

6.7 Zoom on the concentration field for a single channel. Simulation conditions: $u_{\text{in}} = 0.1m/s$, $\Delta P = \Delta P1$. 50

Abstract

We consider the coupled Navier-Stokes/advection-diffusion equations, with nonlinear conditions across a semi-permeable membrane. This system of partial differential equations arises from reverse osmosis modeling in water desalination processes. To solve the Navier-Stokes equations, we use a conservative hybridizable discontinuous Galerkin (HDG) scheme in primal form. For the advection-diffusion equation, we also employ an HDG method in the primal form. The main advantage of our formulation, in addition to the conservative property, is the fact that the size of the global linear system to solve is smaller compared to non-hybrid schemes for high-order approximations. We show that the scheme is well-posed under smallness assumptions on the data, obtain error estimates and present numerical experiments illustrating the performance of the scheme.

CHAPTER 1

Introduction

Membrane-based desalination methods have gained attention during the last decade due to their low energy consumption compared to thermal-based techniques. In particular, the reverse osmosis process is nowadays one of the most widely used techniques in water desalination plants [8]. Seawater flows into a channel (called the feed channel) at high pressure, and passes through the pores of a semi-permeable membrane. The membrane is capable of retaining colloidal matter and dissolved particles larger than $0.1 - 1.0$ nm. Then, after passing through the membrane, the "almost" pure water is collected in another channel (called the permeate channel).

The mathematical model includes the Navier-Stokes equations for fluid flow along with an advection-diffusion equation for salt concentration. In addition, the feed and permeate channels are coupled by an interface (the semi-permeate membrane) with nonlinear transmission conditions. Solving this nonlinear coupled system is computationally expensive and therefore simulations that consider a single channel are preferred. To be more precise, let Ω be a bounded polygonal domain in $\mathbb{R}^2$ with boundary $\partial\Omega$ as shown in Figure 1.1 and suppose the boundary can be partitioned into an input Γ_{in}, an output Γ_{out}, and two portions describing the membrane, denoted by Σ, i.e., $\partial\Omega = \overline{\Gamma}_{\text{in}} \cup \overline{\Gamma}_{\text{out}} \cup \overline{\Sigma}$. In addition, we denote by $\mathbf{n}$ the outward unit normal vector in $\partial\Omega$ and by $\boldsymbol{m}_\Sigma$ the unit tangent vector in Σ with the orientation depicted in Figure 1.1.

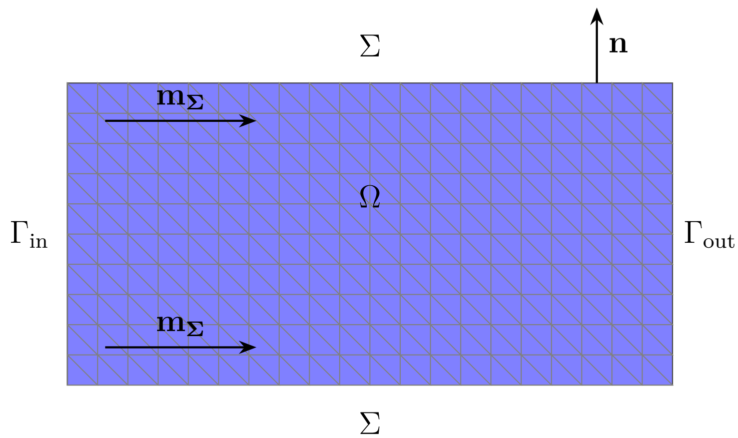

Figure 1.1: Depicting of a single desalination channel.

We consider the following coupled system of equations

$$
\begin{aligned}
-2\mu\nabla\cdot\varepsilon(\boldsymbol{u}) + \rho(\nabla\boldsymbol{u})\boldsymbol{u} + \nabla p = 0, \quad \nabla\cdot\boldsymbol{u} = 0 \quad \text{in} \quad \Omega, \\
-\theta\,\Delta\phi + \boldsymbol{u}\cdot\nabla\phi = 0 \quad \text{in} \quad \Omega,
\end{aligned}
\tag{1.0.1a}
$$

where $\boldsymbol{u}$ is the fluid velocity, $\varepsilon(\boldsymbol{u}) := \frac{1}{2}(\nabla\boldsymbol{u}+\nabla^t\boldsymbol{u})$ is the deformation tensor, p the fluid pressure and ϕ is the concentration of the salt occupying the domain Ω. The given data are the fluid dynamic viscosity μ, the fluid density ρ and the solute diffusivity through the solvent θ. All these parameters are positive constants.

Inlet and outlet boundaries At the inlet boundary Γ_{in}, we consider a given velocity profile $\boldsymbol{u}_{in}$ and a constant concentration ϕ_{in}. At the channel outlet, denoted by Γ_{out}, we consider a do-nothing boundary condition and zero salt diffusion. That is,

$$
\boldsymbol{u} = \boldsymbol{u}_{\text{in}}, \quad \phi = \phi_{\text{in}} \quad \text{on} \quad \Gamma_{\text{in}} \quad \text{and} \quad (2\mu\varepsilon(\boldsymbol{u}) - p\mathbb{I})\mathbf{n} = \mathbf{0}, \quad \nabla\phi\cdot\mathbf{n} = 0 \quad \text{on} \quad \Gamma_{\text{out}}. \tag{1.0.1b}
$$

Imperfect membrane boundary conditions. The semi-permeable membrane is located at the horizontal boundaries of the domain, where the velocity and salt concentration are coupled by the following conditions [3]:

$$\boldsymbol{u}\cdot\boldsymbol{m}_\Sigma = 0, \quad \boldsymbol{u}\cdot\mathbf{n} = c_0 - c_1\,\phi\,, \quad (\phi\boldsymbol{u} - \theta\nabla\phi)\cdot\mathbf{n} \,=\, c_2\phi \quad \text{on} \quad \Sigma,$$

where $c_0 := A\Delta P$, $c_1 := AiRT$ and $c_2 := B$ are known positive constants. Here, B is the salt permeability of the membrane, A the water permeability of the membrane, ΔP the hydrostatic transmembrane pressure, T the temperature of the system, R the ideal gas constant and i the number of ions in the salt solution. Examples of values for these parameters in realistic simulations are given in Table 6.5 of the numerical experiments section. After some algebraic manipulations, we conveniently rewrite these conditions as :

$$\boldsymbol{u}\cdot\boldsymbol{m}_\Sigma = 0, \quad \boldsymbol{u}\cdot\mathbf{n} = c_0 - c_1\phi\,, \quad \theta\nabla\phi\cdot\mathbf{n} + c_1\phi^2 + c_3\phi \,=\, 0 \quad \text{on} \quad \Sigma, \tag{1.0.1c}$$

where $c_3 = c_2 - c_0$.

This coupled system of partial differential equations is usually solved by CFD models, but in the literature there is a lack of a theoretical stability and convergence analysis of the numerical schemes. Recent publications have addressed this topic from the numerical analysis point of view. For example, [3] proposed and analyzed a finite element scheme for a reverse osmosis model using Nitsche's technique. In addition, [2] proposed a conforming mixed finite element method for a coupled Navier–Stokes/advection-diffusion system modeling reverse osmosis processes. The analysis was based on a fixed-point strategy combined for nonlinear perturbations of saddle-point problems. The main drawback of mixed methods is the large number of degrees of freedom required to solve the system. This motivated us to consider a hybridizable scheme in order to reduce the number of globally coupled degrees of freedom. For the Navier-Stokes part, we consider the hybridizable discontinuous Galerkin (HDG) proposed by [16] and then analyzed in [13]. This scheme produces a divergence-free and divergence-conforming approximation of the velocity. For the advection-diffusion equation, we consider the HDG method of [21]. In the literature, we can find conservative HDG schemes for Stokes/Darcy coupling [6, 10], Navier-Stokes/Darcy coupling [5]. To the best of our knowledge, HDG schemes for the coupled Navier-Stokes/advection-diffusion equations with nonlinear boundary conditions have not been developed, and this is one of the main contributions of our work.

1.1 Preliminaries

Sobolev spaces. Given a Lipschitz-continuous domain $\mathcal{O}$ of $\mathbb{R}^2$ with boundary Γ, we adopt standard notations for Lebesgue spaces $L^t(\mathcal{O})$ and Sobolev spaces $W^{l,t}(\mathcal{O})$, with $l \geq 0$ and $t \in [1, +\infty)$, whose corresponding norms, either for the scalar- and vector-valued case, are denoted by $\|\cdot\|_{0,t;\mathcal{O}}$ and $\|\cdot\|_{l,t;\mathcal{O}}$, respectively. Note that $W^{0,t}(\mathcal{O}) = L^t(\mathcal{O})$. If $t = 2$ we write $H^l(\mathcal{O})$ instead of $W^{l,2}(\mathcal{O})$, with the corresponding norm and seminorm denoted by $\|\cdot\|_{l,\mathcal{O}}$ and $|\cdot|_{l,\mathcal{O}}$, respectively. If $l = 0$, i.e., the $L^2(\mathcal{O})$ space, the inner product and the norm will be denoted by $(\cdot,\cdot)_{\mathcal{O}}$ and $\|\cdot\|_{\mathcal{O}}$, resp. Similarly, for functions defined in $L^2(\partial\mathcal{O})$, we write $\langle\cdot,\cdot\rangle_{\partial\mathcal{O}}$ and $\|\cdot\|_{\partial\mathcal{O}}$. $H^{1/2}(\Gamma)$ denotes the space of traces of $H^1(\mathcal{O})$ and $H^{-1/2}(\Gamma)$ its dual space, provided with the duality pairing $\langle\cdot,\cdot\rangle_{\Gamma}$. Also, given $\widetilde{\Gamma} \subseteq \Gamma$, $H^{1/2}(\widetilde{\Gamma})$ denotes the restriction to $\widetilde{\Gamma}$ of $H^1(\mathcal{O})$-functions.

Variational formulation. Given a portion $\widetilde{\Gamma}$ of the boundary and a function g defined on $\widetilde{\Gamma}$, we define the following spaces.

$$H^1_{\widetilde{\Gamma}}(\Omega) := \{v \in H^1(\Omega) : v|_{\widetilde{\Gamma}} = 0\} \quad \text{and} \quad H^1_g(\Omega) := \{v \in H^1(\Omega) : v|_{\widetilde{\Gamma}} = g\}.$$

Let

$$g_\phi := \begin{cases} (c_0 - c_1\phi)\mathbf{n} & \text{on } \Sigma, \\ \boldsymbol{u}_{\text{in}} & \text{on } \Gamma_{\text{in}} \end{cases}$$

and $\Gamma_D := \Gamma_{\text{in}} \cup \Sigma$. We consider the following variational formulation for(1.0.1): Find $(\boldsymbol{u}, p) \in [H^1_{g_\phi}(\Omega)]^2 \times L^2_0(\Omega)$ and $\phi \in H^1_{\phi_{\text{in}}}(\Omega)$, such that

$$(\nu, \varepsilon(\boldsymbol{u}), \varepsilon(\boldsymbol{v}))_\Omega + (\boldsymbol{u}\cdot\nabla\boldsymbol{v}, \boldsymbol{v})_\Omega - (p, \nabla\cdot\boldsymbol{v})_\Omega = 0 \quad \forall \boldsymbol{v} \in [H^1_{\Gamma_D}(\Omega)]^2 \tag{1.1.1a}$$

$$(q, \nabla \cdot \boldsymbol{v})_\Omega = 0 \quad \forall q \in L^2_0(\Omega) \tag{1.1.1b}$$

$$(\theta \nabla \phi, \nabla r)_\Omega + (\boldsymbol{u} \cdot \nabla \phi, r)_\Omega = 0 \quad \forall r \in H^1_{\Gamma_{\mathrm{in}}}(\Omega). \tag{1.1.1c}$$

Showing well-posedeness of (1.1.1) is not trivial due to the nonlinearities and the boundary condition on Σ. This is out of the scope of this thesis, and will be addressed in a future work.

Domain discretization and mesh-dependent inner products We denote by $\{\mathcal{T}\}$ a family of shape-regular triangulations of Ω made of triangles. For simplicity we assume that it is free of hanging-nodes. Given $K \in \mathcal{T}$, we denote by h_K its diameter and n_K its unit outward normal. If there is no confusion, we will write n instead of n_K. Moreover, the set of interior and boundary edges of $\mathcal{T}$ will be denoted by $\mathcal{E}^i$ and $\mathcal{E}^\partial$, resp., and set $\mathcal{E} := \mathcal{E}^i \cup \mathcal{E}^\partial$. Also, if Γ is part of the boundary $\partial\Omega$, $\mathcal{E}^\Gamma$ will denote the partition of Γ induced by $\mathcal{T}$. We define by $\partial\mathcal{T}$ the union of the boundaries of the elements $K \in \mathcal{T}$. The diameter of an element $e \in \mathcal{E}$ will be denoted by h_e.

We also define

$$(\cdot,\cdot)_{\mathcal{T}} := \sum_{K \in \mathcal{T}} (\cdot,\cdot)_K \quad , \quad \langle \cdot,\cdot \rangle_{\partial\mathcal{T}} := \sum_{K \in \mathcal{T}} \langle \cdot,\cdot \rangle_{\partial K} \quad \text{and} \quad \langle \cdot,\cdot \rangle_{\mathcal{E}} := \sum_{e \in \mathcal{E}} \langle \cdot,\cdot \rangle_e \, .$$

where $(\cdot,\cdot)_K$, $\langle \cdot,\cdot \rangle_{\partial K}$ and $\langle \cdot,\cdot \rangle_e$ are the standard L^2- inner products over an element K, its boundary ∂K and face e, respectively.

We denote the trace operator by $\gamma : H^s(\Omega) \to H^{s-1/2}(\partial\mathcal{T})$ to restrict functions in $H^s(\Omega)$ to $\partial\mathcal{T}$. The trace operator is applied component-wise for functions in $[H^s(\Omega)]^2$. We also denote by $\gamma_n : H(\mathrm{div}, \mathcal{T}) \to H^{-1/2}(\partial\mathcal{T})$ the normal trace operator.

Finally, given $k \in \mathbb{N} \cup \{0\}$, we denote by $P_k(K)$ and $P_k(e)$ the spaces of the polynomials of degree at most k defined on $K \in \mathcal{T}$ and $e \in \mathcal{E}$, resp.

L^2-projections. In this thesis, we will work with the following finite-dimensional spaces defined locally over elements of the triangualtion $\mathcal{T}$ (for $k \geq 1$):

$$V_h := \{v_h \in [L^2(\Omega)]^2 \colon v_h \in [P_k(K)]^2, \ \forall \ K \in \mathcal{T}\},$$

$$Q_h := \{q_h \in L^2(\Omega) \quad : q_h \in P_{k-1}(K), \forall\ K \in \mathcal{T}\},$$
$$C_h := \{r_h \in L^2(\Omega) \quad : r_h \in P_k(K), \forall\ K \in \mathcal{T}\},$$

where the subscript h stands for the meshsize $h := \max_{K\in\mathcal{T}} h_K$. Let $W \in \{V_h, Q_h, C_h\}$. Given a function v defined in W, we denote Π_W its L^2-projetion over W. It is well-known that [7], for all $K \in \mathcal{T}$, there exists a constant $C > 0$, independent of h, such that

$$\|v - \Pi_W v\|_K \leq C h_K^s \|v\|_{s,K} \tag{1.1.2}$$

for $s \in \{0, ..., l+1\}$, where l is the polynomial degree of the local spaces that define W.

In addition, for the discretization of the traces, we will consider the finite-dimensional spaces defined on the skeleton $\mathcal{E}$,

$$\bar{V}_h := \{\bar{v}_h \in [L^2(\mathcal{E})]^2\colon\ \bar{v}_h \in [P_k(e)]^2\ \forall\ e \in \mathcal{E}\},$$
$$\bar{Q}_h := \{\bar{q}_h \in L^2(\mathcal{E}) \quad : \bar{q}_h \in P_k(e)\ \forall\ e \in \mathcal{E}\}$$
$$\bar{C}_h := \{\bar{r}_h \in L^2(\mathcal{E}) \quad : \bar{r}_h \in P_k(e)\ \forall\ e \in \mathcal{E}\}.$$

Let $\bar{W} \in \{\bar{V}_h, \bar{Q}_h, \bar{C}_h\}$. Given a function $\bar{v}$ defined in $\overline{W}$, we denote $\overline{\Pi}_W$ its L^2-projetion over $\bar{W}$. It also known that [7], for all $e \in \mathcal{E}$, there exists a constant $C > 0$, independent of h_e, such that

$$\|\bar{v} - \overline{\Pi}_W \bar{v}\|_e \leq C h_e^s \|\bar{v}\|_{s,e} \tag{1.1.3}$$

for $s \in \{0, ..., l+1\}$, where l is the polynomial degree of the local spaces associated to $\bar{W}$.

We end this section by mentioning that we will use the same font to denote scalar-, vector- and tensor-valued functions, depending on the context. Also, to avoid proliferation of unimportant constants, we use the notation $a \lesssim b$ when there exists a positive constant C, independent of h, such that $a \leq C\, b$.

CHAPTER 2

The advection-diffusion equations

In this section, we derive the HDG method for the advection-diffusion equation

$$\nabla \cdot (\phi w - \theta \nabla \phi) = 0 \qquad \text{in } \Omega, \tag{2.0.1a}$$

where w is a given divergence-free velocity field. The boundary $\partial\Omega$ is divided in three disjoint parts: Γ_{out}, Σ and Γ_{in}. In addition, we consider the following boundary conditions

$$\phi = \phi_{\text{in}} \quad \text{on} \;\; \Gamma_{\text{in}}, \tag{2.0.1b}$$

$$\nabla \phi \cdot n = 0 \quad \text{on} \;\; \Gamma_{\text{out}}, \tag{2.0.1c}$$

$$(\phi w - \theta \nabla \phi) \cdot n = c_2 \phi \quad \text{on} \;\; \Sigma, \tag{2.0.1d}$$

where we recall that c_2 is a positive parameter.

Remark 1. It is assumed that $w \cdot n \geq 0$ on the boundary $\Gamma_{\text{out}} \cup \Sigma$. In our application, this is actually the case since water flows out of the channel through the membrane. In fact, from (1.0.1) $u \cdot n = c_0 - c_1 \phi$. The magnitude of the constants c_0 and c_1 are of the order $10^6 A$ and

10^3A, respectively, where we recall that A is the water apermibility of the membrane. Moreover, the magnitude of the inlet concentration ϕ_{in} can take values form 0 to 600.

2.1 An HDG scheme for the Advection-Diffusion Equation equation.

To discretize the advection-diffusion equation (2.0.1b), we consider the 'cell' function space

$$C_h := \{r_h \in L^2(\Omega) : \ r_h \in P_k(K), \ \forall \ K \in \mathcal{T}_h\},$$

and the 'trace' function space

$$\bar{C}_h^g := \{\bar{r}_h \in L^2(\mathcal{E}) : \ \bar{r}_h \in P_k(F) \ , \forall \ F \in \mathcal{F}_h, \ \bar{r}_h = \overline{\Pi}_C g \text{ on } \Gamma_{\text{in}}\},$$

where g is a given function at the boundary Γ_{in} and $\overline{\Pi}_C g$ is the L^2-projection over $\bar{C}_g$ restricted to $\mathcal{E}^{\Gamma_{\text{in}}}$. We set $\boldsymbol{C}_h^g := C_h \times \bar{C}_h^g$. We also write $\boldsymbol{r} := (r, \bar{r}) \in \boldsymbol{C}_h^g$.

Local equations. Given an element $K \in \mathcal{T}$, the outflow $(w \cdot n \geq 0)$ and inflow $(w \cdot n < 0)$ portions of its boundary will be denoted by ∂K^+ and ∂K^-, respectively. We set $\mathcal{T}^{\pm} := \cup_{K \in \mathcal{T}} \partial K^{\pm}$.

Let us denote by ϕ_h the approximation of ϕ. We define $\sigma_\phi := \phi_h w - \theta \nabla \phi_h$ and the corresponding numerical flux

$$\begin{aligned} \hat{\sigma}_\phi \cdot n :=& \phi_h \gamma_n(w) - \zeta \gamma_n(w)(\phi_h - \bar{\phi}_h) - \theta \nabla \phi_h + \frac{\theta \beta^c}{h_K}(\phi_h - \bar{\phi}_h) \\ =& \sigma_\phi \cdot n - \zeta \gamma_n(w)(\phi_h - \bar{\phi}_h) + \frac{\theta \beta^c}{h_K}(\phi_h - \bar{\phi}_h) \end{aligned} \tag{2.1.1}$$

where $\beta^c > 0$ is a penalty parameter, $\bar{\phi}_h$ is the approximation of the trace of ϕ at the skeleton, $\zeta = 0$ on $\partial \mathcal{T}^+$ and $\zeta = 1$ on $\partial \mathcal{T}^-$. We also recall that $\gamma_n(w)$ denotes the normal trace of w over $\partial \mathcal{T}$.

Then, we discretize (2.0.1) as follows:

$$-\sum_{K\in\mathcal{T}}\int_K \sigma_\phi\cdot\nabla r_h\ dx+\sum_{K\in\mathcal{T}}\int_{\partial K}\hat{\sigma}_\phi\cdot n r_h ds=0 \qquad \forall r_h\in C_h. \tag{2.1.2}$$

Global equations. Imposing normal continuity on the numerical flux (2.1.1) and using (2.0.1b), we find for all $\bar{r}_h\in\bar{C}_h$,

$$\sum_{K\in\mathcal{T}}\int_{\partial K}\hat{\sigma}_\phi\cdot n\bar{r}_h\ ds=\int_{\Gamma_{\text{in}}}\sigma_\phi\cdot n\bar{r}_h\ ds+\int_{\Gamma_{\text{out}}}\sigma_\phi\cdot n\bar{r}_h ds+\int_\Sigma \sigma_\phi\cdot n\bar{r}_h ds$$

But, $\bar{r}_h=0$ on Γ_{in}, and $\sigma_\phi\cdot n=\phi\gamma_n(w)$ on Γ_{out} and $\sigma_\phi\cdot n=c_2\phi$ on Σ so that

$$\sum_{K\in\mathcal{T}}\int_{\partial K}\hat{\sigma}_\phi\cdot n\bar{r}_h ds-\int_{\Gamma_{\text{out}}}\gamma_n(w)\bar{\phi}\bar{r}_h ds-\int_\Sigma c_2\bar{\phi}\bar{r}_h ds=0.$$

Combining this expression and (2.1.2),

$$-\sum_{K\in\mathcal{T}}\int_K\sigma_\phi\nabla r_h\,dx+\sum_{K\in\mathcal{T}}\int_{\partial K}\hat{\sigma}_\phi n(r_h-\bar{r}_h)\,ds+\int_{\Gamma_{\text{out}}}\gamma_n(w)\bar{\phi}\,\bar{r}_h\,ds+\int_\Sigma c_2\bar{\phi}\,\bar{r}_h\,ds=0.$$

Now, using the definitions of the fluxes, we obtain

$$\begin{aligned}
&-\sum_{K\in\mathcal{T}}\int_K\phi w\cdot\nabla r_h\,dx+\sum_{K\in\mathcal{T}}\int_K\theta\nabla\phi\cdot\nabla r_h\,dx\\
&+\sum_{K\in\mathcal{T}}\int_{\partial K}(\phi-\zeta(\phi-\bar{\phi}))\gamma_n(w)(r_h-\bar{r}_h)\,ds+\sum_{K\in\mathcal{T}}\int_{\partial K}\frac{\theta\beta^c}{h_K}(\phi-\bar{\phi})(r_h-\bar{r}_h)\,ds\\
&-\sum_{K\in\mathcal{T}}\int_{\partial K}\theta\nabla\phi\cdot n(r_h-\bar{r}_h)\,ds-\sum_{K\in\mathcal{T}}\int_{\partial K}\theta\nabla r_h\cdot n(\phi-\bar{\phi})\,ds\\
&+\int_{\Gamma_{\text{out}}}\gamma_n(w)\bar{\phi}\,\bar{r}_h\,ds+\int_\Sigma c_2\bar{\phi}\,\bar{r}_h\,ds=0.
\end{aligned}$$

Let us introduce the forms

$$o_h^c(w;\boldsymbol{\phi},\boldsymbol{r}):=-\,(\phi w,\nabla r)_{\mathcal{T}}+\langle(\phi-\zeta(\phi-\bar{\phi}))\,\gamma_n(w),r-\bar{r}\rangle_{\partial\mathcal{T}}+\langle\bar{\phi}\gamma_n(w),\bar{r}\rangle_{\Gamma_{\text{out}}}, \tag{2.1.3a}$$

$$\begin{aligned}
a_h^c(\boldsymbol{\phi},\boldsymbol{r}):=\ &(\theta\nabla\phi,\nabla r)_{\mathcal{T}}+\langle\theta\beta^c h_K^{-1}(\phi-\bar{\phi}),r-\bar{r}\rangle_{\partial\mathcal{T}}\\
&-\langle\theta\nabla\phi\cdot n,r-\bar{r}\rangle_{\partial\mathcal{T}}-\langle\theta\nabla r\cdot n,\phi-\bar{\phi}\rangle_{\partial\mathcal{T}}.
\end{aligned} \tag{2.1.3b}$$

The HDG scheme to discretize (2.0.1) reads: Find $\boldsymbol{\phi}_h \in \boldsymbol{C}_h^{\phi_{\text{in}}}$ such that, for all $\boldsymbol{r}_h \in \boldsymbol{C}_h^0$,

$$o_h^c(w; \boldsymbol{\phi}_h, \boldsymbol{r}_h) + a_h^c(\boldsymbol{\phi}_h, \boldsymbol{r}_h) + \langle c_2 \bar{\phi}_h, \bar{r}_h \rangle_\Sigma = 0. \tag{2.1.4}$$

Lemma 2.1.1 (Consistency)**.** *Let $\boldsymbol{\phi} = (\phi, \gamma(\phi))$, with $\phi \in H^2(\Omega)$, a solution of (2.0.1) then*

$$o_h^c(w; \boldsymbol{\phi}, \boldsymbol{r}_h) + a_h^c(\boldsymbol{\phi}, \boldsymbol{r}_h) + \langle c_2 \gamma(\phi), \bar{r}_h \rangle_\Sigma = 0 \quad \forall \boldsymbol{r}_h \in \boldsymbol{C}_h^0.$$

Proof. Let $\boldsymbol{\phi} = (\phi, \gamma(\phi))$ with $\phi \in H^2(\Omega)$ a solution of (1.0.1a). Then, by (2.1.4) we obtain

$$\begin{aligned} o_h^c(w; \boldsymbol{\phi}, \boldsymbol{r}_h) + a_h^c(\boldsymbol{\phi}, \boldsymbol{r}_h) + \langle c_2 \gamma(\phi), \bar{r}_h \rangle_\Sigma = &- \sum_{K \in \mathcal{T}} \int_K \phi w \cdot \nabla r_h \, dx + \sum_{K \in \mathcal{T}} \int_K \theta \nabla \phi \cdot \nabla r_h \, dx \\ &+ \sum_{K \in \mathcal{T}} \int_{\partial K} \phi \gamma_n(w)(r_h - \bar{r}_h) \, ds - \sum_{K \in \mathcal{T}} \int_{\partial K} \theta \nabla \phi \cdot n(r_h - \bar{r}_h) \, ds + \int_\Sigma c_2 \bar{\phi} \bar{r}_h \, ds \\ &+ \int_{\Gamma_{\text{out}}} \gamma_n(w) \bar{\phi} \bar{r}_h \, ds. \end{aligned}$$

We now analyze the case $\boldsymbol{r}_h = (r_h, 0)$. Integrating by parts we have that

$$o_h^c(w; \boldsymbol{\phi}, (r_h, 0))) + a_h^c(\boldsymbol{\phi}, (r_h, 0)) = - \sum_K \int_K \phi w \cdot \nabla r_h \, dx + \sum_K \int_{\partial K} \phi \gamma_n(w) r_h \, ds - \sum_K \int_K \theta \nabla \cdot (\nabla \phi) r_h \, dx.$$

Integrating by parts the first term,

$$o_h^c(w; \boldsymbol{\phi}, (r_h, 0))) + a_h^c(\boldsymbol{\phi}, (r_h, 0)) = \sum_K \int_K \nabla \cdot (\phi w) r_h \, dx - \sum_K \int_K \theta \nabla \cdot (\nabla \phi) r_h \, dx = 0.$$

On the other hand, for the case $\boldsymbol{r}_h = (0, \bar{r}_h)$, we have that

$$\begin{aligned} &- \sum_{K \in \mathcal{T}} \int_{\partial K} \phi \gamma_n(w) \bar{r}_h \, ds + \sum_{K \in \mathcal{T}} \int_{\partial K} \theta \nabla \phi \cdot n \bar{r}_h \, ds + \int_\Sigma c_2 \phi \bar{r}_h \, ds + \int_{\Gamma_{\text{out}}} \gamma_n(w) \phi \bar{r}_h \, ds \\ &= - \int_{\Gamma_{\text{out}}} \phi \gamma_n(w) \bar{r}_h \, ds - \int_\Sigma \phi \gamma_n(w) \bar{r}_h \, ds + \sum_{K \in \mathcal{T}} \int_{\partial K} \theta \nabla \phi \cdot n \bar{r}_h \, ds + \int_\Sigma c_2 \phi \bar{r}_h \, ds + \int_{\Gamma_{\text{out}}} \gamma_n(w) \phi \bar{r}_h \, ds \\ &= - \int_\Sigma \phi \gamma_n(w) \bar{r}_h \, ds + \int_\Sigma \theta \nabla \phi \cdot n \bar{r}_h \, ds + \int_{\Gamma_{\text{out}}} \theta \nabla \phi \cdot n \bar{r}_h \, ds + \int_\Sigma c_2 \phi \bar{r}_h \, ds = 0. \end{aligned}$$

Finally, we conclude that the scheme is consistent after combining both cases. □

In order to deal with homogeneous Dirichlet boundary conditions, and considering the fact that ϕ_{in} is constant, we define $\boldsymbol{z}^c := \boldsymbol{\phi}_h - \boldsymbol{\phi}_{\text{in}}$, where $\boldsymbol{\phi}_{\text{in}} := (\phi_{\text{in}}, \phi_{\text{in}})$.

Then we can write (2.1.4) as: Find $\boldsymbol{z}^c \in \boldsymbol{C}_h^0$ such that:

$$A^c(\boldsymbol{z}^c, \boldsymbol{r}) = F(\boldsymbol{r}) \qquad \forall \boldsymbol{r} \in \boldsymbol{C}_h^0, \tag{2.1.5}$$

where $F(\boldsymbol{r}) := -o_h^c(w; \boldsymbol{\phi}_{\text{in}}, \boldsymbol{r}) - a_h^c(\boldsymbol{\phi}_{\text{in}}, \boldsymbol{r}) - \langle c_2\phi_{\text{in}}, \bar{r}_h\rangle_\Sigma = \langle \phi_{\text{in}}(c_2 - \gamma_n(w)), \bar{r}\rangle_\Sigma$.

2.2 Well-posedness.

Our analysis will be based on the arguments provided in [21]. Let us introduce the spaces

$$C^*(h) := C_h + H^1_{\Gamma_{\text{in}}}(\Omega), \quad \bar{C}^*(h) := \bar{C}_h^0 + H^{3/2}_{\Gamma_{\text{in}}}(\partial\mathcal{T}_h) \tag{2.2.1}$$

and $\boldsymbol{C}^*(h) := C^*(h) \times \bar{C}^*(h)$, where $H^1_{\Gamma_{\text{in}}}(\Omega)$ is the space of $H^1(\Omega)$-functions with zero trace on Γ_{in} and $H^{3/2}_{\Gamma_{\text{in}}}(\partial\mathcal{T}_h)$ is the trace space of $H^1_{\Gamma_{\text{in}}}(\Omega) \cap H^2(\Omega)$. We also consider the following norms for a function $\boldsymbol{r} = (r, \bar{r}) \in \boldsymbol{C}^*(h)$:

$$\begin{aligned}
|\!|\!|\boldsymbol{r}|\!|\!|_D &:= \left(\|\theta^{1/2}\nabla r\|^2_{\mathcal{T}} + \|\theta^{1/2}h_K^{-1/2}(r - \bar{r})\|^2_{\partial\mathcal{T}}\right)^{1/2} \\
|\!|\!|\boldsymbol{r}|\!|\!|_t &:= \left(|\!|\!|\boldsymbol{r}|\!|\!|^2_D + \||\gamma_n(w)|^{1/2}(r - \bar{r})\|^2_{\partial\mathcal{T}} + \||\gamma_n(w)|^{1/2}\bar{r}\|^2_{\Gamma_{\text{out}}} + c_2\|\bar{r}\|^2_{\Sigma\cup\Gamma_{\text{out}}}\right)^{1/2}, \\
|\!|\!|\boldsymbol{r}|\!|\!|_A &:= \left(|\!|\!|\boldsymbol{r}|\!|\!|^2_t + \sum_{K\in\mathcal{T}} h_K\|w\cdot\nabla r\|^2_{0,K}\right)^{1/2}, \\
|\!|\!|\boldsymbol{r}|\!|\!|_{A'} &:= \left(|\!|\!|\boldsymbol{r}|\!|\!|^2_A + \sum_{K\in\mathcal{T}} h_K^{-1}\|w\cdot\nabla r\|^2_{0,K} + \sum_{K\in\mathcal{T}}\||\gamma_n(w)|^{1/2}\bar{r}\|^2_{0,\partial K^-} + \sum_{K\in\mathcal{T}}\||\gamma_n(w)|^{1/2}r\|^2_{0,\partial K^+}\right)^{1/2},
\end{aligned}$$

where w is a given velocity. Furthermore, the following discrete Poincaré inequality holds [7, Theorem 5.3]:

$$\|r\|_{\mathcal{T}} \le c_p\|r\|_{1,h} \le c_p|\!|\!|\boldsymbol{r}|\!|\!|_s \quad \forall \boldsymbol{r} \in \boldsymbol{C}_h^0, \tag{2.2.2}$$

where c_p is a constant independent of h_K. In addition, according to [12, Theorem 4.4], there exists $c_{tr} > 0$, independent of the meshsize, such that

$$\|r\|_{0,r,\Sigma} \leq c_{tr} \| \boldsymbol{r} \|_D \quad \forall \boldsymbol{r} \in \boldsymbol{C}_h^0 \tag{2.2.3}$$

and $r \geq 2$.

Lemma 2.2.1. *Let $w \in V_h \cap H(\mathrm{div};\Omega)$. There exist positive constants M_o, M_a, M_A and M_4, independent of h, such that,*

$$o_h^c(w;\boldsymbol{v},\boldsymbol{r}) \leq M_4 \|w\|_{0,4,\Omega} \| \boldsymbol{v} \|_D \| \boldsymbol{r} \|_D \quad \forall \boldsymbol{v} \in [H^1(\mathcal{T}_h)]^2 \times [L^2(\mathcal{E})]^2, \forall \boldsymbol{r} \in \boldsymbol{C}_h^0 \tag{2.2.4a}$$

$$a_h^c(\boldsymbol{v},\boldsymbol{r}) \leq M_a \| \boldsymbol{v} \|_{D'} \| \boldsymbol{r} \|_D \quad \forall \boldsymbol{v} \in \boldsymbol{C}^*(h), \forall \boldsymbol{r} \in \boldsymbol{C}_h^0, \tag{2.2.4b}$$

$$A^c(\boldsymbol{v},\boldsymbol{r}) \leq M_A \| \boldsymbol{v} \|_D \, \| \boldsymbol{r} \|_D \quad \forall \boldsymbol{v}, \boldsymbol{r} \in \boldsymbol{C}^*(h). \tag{2.2.4c}$$

where $M_A = \max\{M_4\|w\|_{0,4,\Omega} + M_a, 1\}$ and

$$A^c(\boldsymbol{v},\boldsymbol{r}) := o_h^c(w;\boldsymbol{r},\boldsymbol{v}) + a_h^c(\boldsymbol{v},\boldsymbol{r}) + \langle c_2\bar{v},\bar{r}\rangle_\Sigma.$$

In addition, if $w \in V_h \cap H(\mathrm{div},\Omega)$ and $w|_{\Gamma_{\mathrm{in}}} = 0$, then

$$o_h^c(w;\boldsymbol{v},\boldsymbol{r}) \leq M_o \|w\|_{1,h} \| \boldsymbol{v} \|_D \| \boldsymbol{r} \|_D \quad \forall \boldsymbol{v} \in [H^1(\mathcal{T}_h)]^2 \times [L^2(\mathcal{E})]^2, \forall \boldsymbol{r} \in \boldsymbol{C}_h^0, \tag{2.2.4d}$$

where $\|w\|_{1,h} := \| (w,\{w\}) \|_D$.

Proof. Inequalities (2.2.4a) and (2.2.4d) can be obtained by the same arguments as in the proof of Proposition 3.4 in [4], but now considering that $\bar{r}$ vanishes in part of the boundary. Estimate (2.2.4b) has been shown in Lemma 4.3 of [14]. The last inequality is a consequence of the other two.

□

Lemma 2.2.2. *Let $w \in H(\mathrm{div}, \Omega)$ be divergence-free and $\boldsymbol{r} \in H^1(\mathcal{T}) \times L^2(\mathcal{E})$. It holds*

$$o_h^c(w; \boldsymbol{r}, \boldsymbol{r}) = \frac{1}{2}\||\gamma_n(w)|^{1/2}(r - \bar{r})\|^2_{\partial\mathcal{T}} - \frac{1}{2}\langle \gamma_n(w), \bar{r}^2\rangle_{\partial\Omega} + \langle \gamma_n(w), \bar{r}^2\rangle_{\Gamma_{\mathrm{out}}}. \tag{2.2.5a}$$

Moreover, if β^c is sufficiently large, there exists $C_a^t > 0$, independent of h, such that

$$a_h^c(\boldsymbol{r}, \boldsymbol{r}) \geq C_a^t \|\boldsymbol{r}\|_D^2 \quad \forall \boldsymbol{r} \in \boldsymbol{C}_h^0. \tag{2.2.5b}$$

In addition, if $\|\gamma_n(w)\|_\Sigma \leq C_a^t/(2c_{st})$, with c_{st} a positive constant independent of h appearing in the proof, then

$$A^c(\boldsymbol{r}, \boldsymbol{r}) \geq C^\dagger \|\boldsymbol{r}\|_D^2 \qquad \forall \boldsymbol{r} \in \boldsymbol{C}_h^0, \tag{2.2.5c}$$

where $C^\dagger := C_a^t/2$.

Proof. Let $w \in H(\mathrm{div}, \Omega)$ be divergence-free and $\boldsymbol{r} \in H^1(\mathcal{T}) \times L^2(\mathcal{E})$. We have $(rw, \nabla r)_\mathcal{T} = \frac{1}{2}\langle \gamma_n(w)\, r, r\rangle_\mathcal{T}$; and recalling that $\zeta = 0$ on $\mathcal{T}^+$ and $\zeta = 1$ on $\mathcal{T}^-$, we have

$$\begin{aligned}
o_h^c(w; \boldsymbol{r}, \boldsymbol{r}) &= -\frac{1}{2}\langle r\,\gamma_n(w), r\rangle_{\partial\mathcal{T}} + \langle r\,\gamma_n(w), r - \bar{r}\rangle_{\partial\mathcal{T}^+} + \langle \bar{r}\,\gamma_n(w), r - \bar{r}\rangle_{\partial\mathcal{T}^-} + \langle \bar{r}\gamma_n(w), \bar{r}\rangle_{\Gamma_{\mathrm{out}}} \\
&= -\frac{1}{2}\langle \gamma_n(w), r^2\rangle_{\partial\mathcal{T}^+} - \frac{1}{2}\langle \gamma_n(w), r^2\rangle_{\partial\mathcal{T}^-} + \langle \gamma_n(w), r^2 - \bar{r}r\rangle_{\partial\mathcal{T}^+} \\
&\quad + \langle \gamma_n(w), \bar{r}r - \bar{r}^2\rangle_{\partial\mathcal{T}^-} + \||\gamma_n(w)|^{1/2}\bar{r}\|^2_{\Gamma_{\mathrm{out}}} \\
&= \frac{1}{2}\langle \gamma_n(w), r^2 - 2\bar{r}r\rangle_{\partial\mathcal{T}^+} - \frac{1}{2}\langle \gamma_n(w), -2\bar{r}r + 2\bar{r}^2 + r^2\rangle_{\partial\mathcal{T}^-} + \||\gamma_n(w)|^{1/2}\bar{r}\|^2_{\Gamma_{\mathrm{out}}} \\
&= \frac{1}{2}\langle \gamma_n(w), (r - \bar{r})^2\rangle_{\partial\mathcal{T}^+} - \frac{1}{2}\langle \gamma_n(w), \bar{r}^2\rangle_{\partial\mathcal{T}^+} - \frac{1}{2}\langle \gamma_n(w), (r - \bar{r})^2)\rangle_{\partial\mathcal{T}^-} \\
&\quad - \frac{1}{2}\langle \gamma_n(w), \bar{r}^2\rangle_{\partial\mathcal{T}^-} + \||\gamma_n(w)|^{1/2}\bar{r}\|^2_{\Gamma_{\mathrm{out}}} \\
&= \frac{1}{2}\||\gamma_n(w)|^{1/2}(r - \bar{r})\|^2_{\partial\mathcal{T}} - \frac{1}{2}\langle \gamma_n(w), \bar{r}^2\rangle_{\partial\mathcal{T}} + \||\gamma_n(w)|^{1/2}\bar{r}\|^2_{\Gamma_{\mathrm{out}}}.
\end{aligned}$$

Since $w \in H(\mathrm{div}, \Omega)$ and $\bar{r}$ is single-valued and vanishes in Γ_{in}, we obtain (2.2.5a).

On the other hand, let $\boldsymbol{r} \in \boldsymbol{C}_h^0$. We have that

$$a_h^c(\boldsymbol{r}, \boldsymbol{r}) = \|\theta^{1/2}\nabla r\|^2_\mathcal{T} + \|(\theta\beta^c)^{1/2} h_K^{-1/2}(r - \bar{r})\|^2_{\partial\mathcal{T}} - 2\langle \theta\nabla r \cdot n, r - \bar{r}\rangle_{\partial\mathcal{T}}.$$

By the discrete trace inequality, there exists $C_{tr} > 0$, such that

$$\begin{aligned}
|2\langle\theta\nabla r\cdot n, r-\bar{r}\rangle_{\partial\mathcal{T}}| &\le 2\sum_{T\in\mathcal{T}}\theta\|\nabla r\cdot n\|_{0,\partial T}\|r-\bar{r}\|_{0,\partial T}\\
&\le 2C_{tr}\sum_{T\in\mathcal{T}}\|\theta^{1/2}\nabla r\cdot n\|_{0,T}\|\theta^{1/2}h_K^{-1/2}(r-\bar{r})\|_{0,\partial T}\\
&\le \sum_{T\in\mathcal{T}}\frac{1}{2}\|\theta^{1/2}\nabla r\|^2_{0,T}+\kappa\sum_{T\in\mathcal{T}}\|\theta^{1/2}h_K^{-1/2}(r-\bar{r})\|^2_{0,\partial T}\\
&\le \frac{1}{2}\|\theta^{1/2}\nabla r\|^2_{\mathcal{T}}+C_{tr}^2\|\theta^{1/2}h_K^{-1/2}(r-\bar{r})\|^2_{0,\partial\mathcal{T}}.
\end{aligned}$$

Then,

$$a_h^c(\boldsymbol{r},\boldsymbol{r}) \ge \frac{1}{2}\|\theta^{1/2}\nabla r\|^2_{\mathcal{T}}+\|\theta^{1/2}((\beta^c)^{1/2}-C_{tr})h_K^{-1/2}(r-\bar{r})\|^2_{\partial\mathcal{T}},$$

which implies (2.2.5b).

Finally, since $A^c(\boldsymbol{r},\boldsymbol{r}) = a_h^c(\boldsymbol{r},\boldsymbol{r}) + o_h^c(w;\boldsymbol{r},\boldsymbol{r}) + \||\gamma_n(w)|^{1/2}\bar{r}\|^2_{\Gamma_{\text{out}}} + c_2\|\bar{r}\|^2_{\Sigma}$,

$$\begin{aligned}
A^c(\boldsymbol{r},\boldsymbol{r}) =& a_h^c(\boldsymbol{r},\boldsymbol{r}) + o_h^c(w;\boldsymbol{r},\boldsymbol{r}) + \||\gamma_n(w)|^{1/2}\bar{r}\|^2_{\Gamma_{\text{out}}} + c_2\|\bar{r}\|^2_{\Sigma}\\
=& a_h^c(\boldsymbol{r},\boldsymbol{r}) + \frac{1}{2}\||\gamma_n(w)|^{1/2}\bar{r}\|^2_{\Gamma_{\text{out}}} - \frac{1}{2}\||\gamma_n(w)|^{1/2}\bar{r}\|^2_{\Sigma} + c_2\|\bar{r}\|^2_{\Sigma}\\
\ge& C_a^t\|\boldsymbol{r}\|^2_D + \frac{1}{2}\||\gamma_n(w)|^{1/2}\bar{r}\|^2_{\Gamma_{\text{out}}} - \frac{1}{2}\||\gamma_n(w)|^{1/2}\bar{r}\|^2_{\Sigma} + c_2\|\bar{r}\|^2_{\Sigma}\\
\ge& C_a^t\|\boldsymbol{r}\|^2_D - \frac{1}{2}\||\gamma_n(w)|^{1/2}\bar{r}\|^2_{\Sigma},
\end{aligned} \tag{2.2.6}$$

where we have used (2.2.5a) and (2.2.5b).

Now, following the arguments in the proof of Lemma 6 of [5], we have that

$$\begin{aligned}
\||\gamma_n(w)|^{1/2}\bar{r}\|^2_{\Sigma} \le& 2\||\gamma_n(w)|^{1/2}(r-\bar{r})\|^2_{\Sigma} + 2\||\gamma_n(w)|^{1/2}r\|^2_{\Sigma}\\
=& 2\sum_{e\in\mathcal{E}^\Sigma}\int_e|\gamma_n(w)|(r-\bar{r})^2 + 2\sum_{e\in\mathcal{E}^\Sigma}\int_e|\gamma_n(w)|r^2\\
\le& 2\sum_{e\in\mathcal{E}^\Sigma}\|\gamma_n(w)\|_e\|r-\bar{r}\|^2_{0,4,e} + 2\sum_{e\in\mathcal{E}^\Sigma}\|\gamma_n(w)\|_e\|r\|^2_{0,4,e}.
\end{aligned}$$

By a scaling argument, it is possible to show that there exists $c^e_{sc,1} > 0$, independent of h, such that $\|\mu\|_{0,4,e} \leq c^e_{sc,1}\, h_e^{-1/4}\|\mu\|_{0,e}$, for all μ in finite dimension. Then,

$$\begin{aligned}\||\gamma_n(w)|^{1/2}\bar{r}\|^2_\Sigma \leq & 2\sum_{e\in\mathcal{E}^\Sigma}(c^e_{sc,1})^2\|\gamma_n(w)\|_e h_e^{-1/2}\|r-\bar{r}\|^2_{0,e} + 2\sum_{e\in\mathcal{E}^\Sigma}\|\gamma_n(w)\|_e\|r\|^2_{0,4,e}\\ \leq & 2c^2_{sc,1}\|\gamma_n(w)\|_\Sigma \,\|\boldsymbol{r}\|^2_D + 2\|\gamma_n(w)\|_\Sigma\,\|r\|^2_{0,4,\Sigma},\end{aligned}$$

where $c_{sc,1} = \max_{e\subset\Sigma} c^e_{sc,1}$. To bound the last term we use (2.2.3), and obtain

$$\||\gamma_n(w)|^{1/2}\bar{r}\|^2_\Sigma \leq 2(c^2_{sc,1}+c^2_{tr})\|\gamma_n(w)\|_\Sigma\,\|\boldsymbol{r}\|^2_D. \tag{2.2.7}$$

Thus, replacing this inequality in (2.2.6), we have

$$A^c(\boldsymbol{r},\boldsymbol{r}) \geq \left(C^t_a - c_{sc}\|\gamma_n(w)\|_\Sigma\right)\|\boldsymbol{r}\|^2_D$$

with $c_{sc} = 2(c^2_{sc,1}+c^2_{tr})$. The result is derived from the fact that $\|\gamma_n(w)\|_\Sigma$ is small enough. □

Theorem 2.2.3. *If $\|\gamma_n(w)\|_\Sigma \leq C^t_a/(2c_{st})$, then the HDG scheme (2.1.5) (equivalently (2.1.4)) is well-posed. Moreover,*

$$\|\boldsymbol{\phi}_h\|_D \leq C_T\|\phi_{\rm in}(c_2-\gamma_n(w))\|_\Sigma. \tag{2.2.8a}$$

and

$$\|\bar{\phi}_h\|_\Sigma \leq \widehat{C}_T\|\phi_{\rm in}(c_2-\gamma_n(w))\|_\Sigma + \|\phi_{\rm in}\|_\Sigma. \tag{2.2.8b}$$

with $C_T := (C^\dagger)^{-1}\max\{\theta^{-1/2}h^{1/2}, c_{tr}\}$ and $\widehat{C}_T := (C^\dagger)^{-1}\max\{\theta^{-1/2}h^{1/2}, c_{tr}\}^2$.

Proof. The bilinear form A^c is bounded and coercive according to Lemma 2.2.1 and (2.2.5a). Moreover, the functional F is bounded. In fact, let $\boldsymbol{r}\in\boldsymbol{C}^0_h$.

$$F(\boldsymbol{r}) := \langle\phi_{\rm in}(c_2-\gamma_n(w)),\bar{r}\rangle_\Sigma \leq \|\phi_{\rm in}(c_2-\gamma_n(w))\|_\Sigma\|\bar{r}\|_\Sigma.$$

Now, according to [12, Theorem 4.4], there exists $c_{tr} > 0$, independent of h, such that

$$\|r\|_\Sigma \le c_{tr} |\!|\!| \boldsymbol{r} |\!|\!|_D \quad \forall \boldsymbol{r} \in \boldsymbol{C}_h^0. \tag{2.2.9}$$

Then,

$$\|\bar{r}\|_\Sigma \le \|r - \bar{r}\|_\Sigma + \|r\|_\Sigma \le \max\{\theta^{-1/2} h^{1/2}, c_{tr}\} |\!|\!| \boldsymbol{r} |\!|\!|_D \quad \forall \boldsymbol{r} \in \boldsymbol{C}_h^0 \tag{2.2.10}$$

and

$$F(\boldsymbol{r}) \le \max\{\theta^{-1/2} h^{1/2}, c_{tr}\} \|\phi_{\text{in}}(c_2 - \gamma_n(w))\|_\Sigma |\!|\!| \boldsymbol{r} |\!|\!|_D.$$

Therefore, by the Lax-Milgram lemma, we conclude that the HDG scheme (2.1.5) has a unique solution. In addition, by the ellipticity property (2.2.5c), we have that

$$C^\dagger |\!|\!| \boldsymbol{z}^c |\!|\!|_D^2 \le A^c(\boldsymbol{z}^c, \boldsymbol{z}^c) = F(\boldsymbol{z}^c) \le \max\{\theta^{-1/2} h^{1/2}, c_{tr}\} \|\phi_{\text{in}}(c_2 - \gamma_n(w))\|_\Sigma \|_{\Gamma_{\text{in}}} |\!|\!| \boldsymbol{z}^c |\!|\!|_D.$$

Then,

$$|\!|\!| \boldsymbol{z}^c |\!|\!|_D \le (C^\dagger)^{-1} \max\{\theta^{-1/2} h^{1/2}, c_{tr}\} \|\phi_{\text{in}}(c_2 - \gamma_n(w))\|_\Sigma.$$

The first statement follows after noting that $|\!|\!| \boldsymbol{\phi}_h |\!|\!|_D = |\!|\!| \boldsymbol{z}^c |\!|\!|_D$. Finally, by (2.2.10) and the previous estimate,

$$\begin{aligned}
\|\bar{\phi}_h\|_\Sigma \le & \|\bar{\phi}_h - \phi_{\text{in}}\|_\Sigma + \|\phi_{\text{in}}\|_\Sigma \\
\le & \max\{\theta^{-1/2} h^{1/2}, c_{tr}\} |\!|\!| \boldsymbol{z}^c |\!|\!|_D + \|\phi_{\text{in}}\|_\Sigma \\
\le & (C^\dagger)^{-1} \max\{\theta^{-1/2} h^{1/2}, c_{tr}\}^2 \|\phi_{\text{in}}(c_2 - \gamma_n(w))\|_\Sigma + \|\phi_{\text{in}}\|_\Sigma,
\end{aligned}$$

which implies the last statement. □

CHAPTER 3

The Navier-Stokes equations

This chapter is devoted to the introduction of the HDG scheme used to approximate the solution of the incompressible Navier-Stokes equations in a domain $\Omega \subset \mathbb{R}^2$, that is,

$$\nabla \cdot \sigma = f \qquad \text{in } \Omega, \tag{3.0.1a}$$

$$\nabla \cdot u = 0 \qquad \text{in } \Omega, \tag{3.0.1b}$$

where $\sigma := \sigma_a + \sigma_d$, $\sigma_a := u \otimes u$, $\sigma_d := p\mathbb{I} - 2\nu\varepsilon(u)$, $f \in L^2(\Omega)$ is a source term, $\nu := \mu/\rho > 0$ with μ the fluid dynamic viscosity and ρ the fluid density. We split the boundary $\partial\Omega$ into Dirichlet (Γ_D) and Neumann (Γ_{out}) parts, and consider the following conditions:

$$u = g_D \qquad \text{on } \Gamma_D, \tag{3.0.1c}$$

$$\sigma_d \, n = 0 \qquad \text{on } \Gamma_{\text{out}}, \tag{3.0.1d}$$

where g_D is a given function.

3.1 An HDG scheme for the Navier-Stokes equations.

For the discretization of the Navier-Stokes equations, we introduce the 'cell' function spaces

$$V_h := \{v_h \in [L^2(\Omega)]^2 : \ v_h \in [P_k(K)]^2, \ \forall\ K \in \mathcal{T}\},$$
$$Q_h := \{q_h \in L^2(\Omega) : \ q_h \in P_{k-1}(K), \forall\ K \in \mathcal{T}\},$$

and the 'trace' function spaces

$$\bar{V}_h^g := \{\bar{v}_h \in [L^2(\mathcal{E})]^2 : \ \bar{v}_h \in [P_k(e)]^2 \ \forall\ e \in \mathcal{E}, \ \bar{v}_h = \overline{\Pi}_V g \text{ on } \Gamma_D\},$$
$$\bar{Q}_h := \{\bar{q}_h \in L^2(\mathcal{E}) : \ \bar{q}_h \in P_k(e) \ \forall\ e \in \mathcal{E}\},$$

where g is a given function at the boundary Γ_D and $\overline{\Pi}_V g$ is understood as the $L^2(\mathcal{E})$-projection $\overline{\Pi}_V$ restricted to $\mathcal{E}^{\Gamma_D}$. We set $\boldsymbol{V}_h^g := V_h \times \bar{V}_h^g$ and $\boldsymbol{Q}_h := Q_h \times \bar{Q}_h$.

Given functions $v \in V_h$ and $\bar{v} \in \bar{V}_h^g$, we denote $\boldsymbol{v} := (v, \bar{v}) \in \boldsymbol{V}_h^g$. Similarly, $\boldsymbol{q} := (q, \bar{q}) \in \boldsymbol{Q}_h$ when $q \in Q_h$ and $\bar{q} \in \bar{Q}_h$.

3.1.1 Derivation of the discrete momentum equation.

The local problems. Let us denote by σ_h and u_h the approximations to σ and u, and also set $\sigma_h := \sigma_{a,h} + \sigma_{d,h}$, $\sigma_{a,h} := u_h \otimes u_h$, $\sigma_{d,h} := p_h \mathbb{I} - 2\nu\varepsilon(u_h)$.

Considering (3.0.1a) in an element K, multiplying by a test function $v_h|_K \in P_k(K)$, integrating by parts over K and adding over all the elements, we have the following:

$$\sum_{K\in\mathcal{T}} \int_K (-\sigma_h : \nabla v_h)\ dx + \sum_{K\in\mathcal{T}} \int_{\partial K} v_h \cdot \hat{\sigma}_h n\ ds - \sum_{K\in\mathcal{T}} \int_{\partial K} 2\nu\varepsilon(v_h)n \cdot (u_h - \bar{u}_h)\ ds = \sum_{K\in\mathcal{T}} \int_K f \cdot v_h\ dx, \quad (3.1.1)$$

where the third term on the left-hand side is a consistent symmetrizing term for the diffusive part, $\bar{u}_h$ is an approximation of the trace of u at the skeleton, and $\hat{\sigma}_h$ is a numerical flux on the cell facets to be defined properly. In particular, we set $\hat{\sigma}_h n := \hat{\sigma}_{a,h} n + \hat{\sigma}_{d,h} n$ with the advective part given by

$$\hat{\sigma}_{a,h}n = (u_h \cdot n)\bar{u}_h + \lambda_u(u_h - \bar{u}_h),$$

with λ_u a stabilization parameter to be determined, and the diffusive part defined as

$$\hat{\sigma}_{d,h} := \bar{p}_h\mathbb{I} - 2\nu\varepsilon(u_h) + \frac{2\nu\alpha}{h_K}(u_h - \bar{u}_h) \otimes n,$$

where $\alpha > 0$ is a sufficiently large penalty parameter. Replacing these definitions of the fluxes (3.1.1), we obtain the following.

$$\begin{aligned}
&\sum_{K\in\mathcal{T}}\int_K 2\nu\varepsilon(u_h) : \varepsilon(v_h)\ dx - \sum_{K\in\mathcal{T}}\int_K u_h \otimes u_h : \nabla v_h\ dx - \sum_{K\in\mathcal{T}}\int_K p\nabla v_h\ dx \\
&+ \sum_{K\in\mathcal{T}}\int_{\partial K} v_h\bar{p}\ ds - \sum_{K\in\mathcal{T}}\int_{\partial K} 2\nu\varepsilon(u_h)n \cdot v_h\ ds - \sum_{K\in\mathcal{T}}\int_{\partial K}\frac{2\nu\alpha}{h_K}v_h(u_h - \bar{u}_h)\ ds \\
&+ \sum_{K\in\mathcal{T}}\int_{\partial K} v_h((u_h \cdot n)\bar{u}_h + \lambda_u(u_h - \bar{u}_h))n\ ds - \sum_{K\in\mathcal{T}}\int_{\partial K} 2\nu\varepsilon(v_h)n \cdot (u_h - \bar{u}_h)\ ds \\
&= \sum_{K\in\mathcal{T}}\int_K f v_h\ dx,
\end{aligned} \tag{3.1.2}$$

where $\lambda_u := u_h \cdot n \begin{cases} 1 & \text{if} \quad u_h \cdot n > 0 \\ 0 & \text{if} \quad u_h \cdot n \leq 0 \end{cases}.$

The global problem. To impose continuity of the normal flux, considering the Neumann boundary condition, for all $\bar{v}_h \in \bar{V}_h^0$, we have the following.

$$\sum_{K\in\mathcal{T}}\int_{\partial K}\hat{\sigma}_h n \cdot \bar{v}_h\ ds = \int_{\Gamma_{\text{out}}}\hat{\sigma}_{a,h}n \cdot \bar{v}_h,$$

because $\sigma_d\, n = 0$ on Γ_{out}. Moreover, since $u \cdot n >$ on Γ_{out}, from the above expression we have

$$\sum_{K\in\mathcal{T}}\int_{\partial K}\hat{\sigma}_h n \cdot \bar{v}_h\ ds = \int_{\Gamma_{\text{out}}}(u_h \cdot n)\bar{u}_h\bar{v}_h\ ds,$$

Writing out the definition of the numerical flux $\hat{\sigma}_h$, we obtain

$$
\begin{aligned}
\int_{\Gamma_{\text{out}}} (u_h \cdot n)\bar{u}_h(-\bar{v}_h)\ ds = & \sum_{K\in\mathcal{T}} \int_{\partial K} \bar{p}_h n \cdot (-\bar{v}_h)\ ds - \sum_{K\in\mathcal{T}} \int_{\partial K} 2\nu\varepsilon(u_h)\cdot(-\bar{v}_h)\ ds \\
& + \sum_{K\in\mathcal{T}} \int_{\partial K} \frac{2\nu\alpha}{h_K}(u_h - \bar{u}_h)\cdot(-\bar{v}_h)\ ds \\
& + \sum_{K\in\mathcal{T}} \int_{\partial K} ((u_h\cdot n)\bar{u}_h + \lambda_u(u_h - \bar{u}_h))n(-\bar{v}_h)\ ds
\end{aligned} \tag{3.1.3}
$$

3.1.2 Derivation of the discrete mass equation.

The local problems. Mass conservation (3.0.1b) is imposed by

$$
\sum_{K\in\mathcal{T}} \int_K q_h \nabla\cdot u_h\ dx = 0 \qquad \forall q_h \in Q_h. \tag{3.1.4}
$$

The global problem. The following equation imposes the continuity of the normal component of the velocity field:

$$
0 = \sum_{K\in\mathcal{T}} \int_{\partial K} \bar{q}_h(u_h - \bar{u}_h)\cdot n\ ds \qquad \forall \bar{q}_h \in \bar{Q}_h. \tag{3.1.5}
$$

We end this section by summarizing the equations obtained and writing the HDG scheme in a compact form by introducing the following forms:

$$
\begin{aligned}
a_h^{ns}(\boldsymbol{u},\boldsymbol{v}) :=& (2\nu\varepsilon(u),\varepsilon(v))_{\mathcal{T}} + \langle 2\nu\alpha h_K^{-1}(u-\bar{u}),(v-\bar{v})\rangle_{\partial\mathcal{T}} \\
& - \langle 2\nu(u-\bar{u}),\varepsilon(v)n\rangle_{\partial\mathcal{T}} - \langle 2\nu\varepsilon(u)n,(v-\bar{v})\rangle_{\partial\mathcal{T}} \\
o_h^{ns}(w;\boldsymbol{u},\boldsymbol{v}) :=& -(u\otimes w,\nabla v)_{\mathcal{T}} + \langle((w\cdot n)\bar{u} + \lambda_w(u-\bar{u}))n, v-\bar{v}\rangle_{\partial\mathcal{T}} + \langle(w\cdot n)\bar{u},\bar{v}\rangle_{\Gamma_{\text{out}}} \\
b_h^{ns}(\boldsymbol{q},\boldsymbol{v}) :=& -(q,\nabla\cdot v)_{\mathcal{T}} + \langle\bar{q},(v-\bar{v})\cdot n\rangle_{\partial\mathcal{T}} \\
L_h^{ns}(\boldsymbol{v}) :=& (f,v_h)_{\mathcal{T}},
\end{aligned}
$$

where we recall that $\boldsymbol{u} = (u,\bar{u})$,$\boldsymbol{v} = (v,\bar{v})$, $\boldsymbol{q} = (q,\bar{q})$. Then, adding (3.1.3) and (3.1.2), and subtracting (3.1.4) from (3.1.5), the HDG method reads as follows: Find $(\boldsymbol{u}_h,\boldsymbol{p}_h) \in \boldsymbol{V}_h^{u_D} \times \boldsymbol{Q}_h$

such that

$$a_h^{ns}(\boldsymbol{u}_h, \boldsymbol{v}_h) + o_h^{ns}(u_h; \boldsymbol{u}_h, \boldsymbol{v}_h) + b_h^{ns}(\boldsymbol{p}_h, \boldsymbol{v}_h) = L_h^{ns}(\boldsymbol{v}_h) \qquad \forall \boldsymbol{v}_h \in \boldsymbol{V}_h^0, \tag{3.1.6a}$$

$$b_h^{ns}(\boldsymbol{q}_h, \boldsymbol{u}_h) = 0 \qquad \forall \boldsymbol{q}_h \in \boldsymbol{Q}_h. \tag{3.1.6b}$$

This scheme has the following mass conservation property [16, Proposition 1]:

$$\nabla \cdot u_h = 0 \qquad \forall K \in \mathcal{T}, \tag{3.1.7a}$$

$$(u_h^+ \cdot n^+ + u_h^- \cdot n^-)|_e = 0 \qquad \forall e \in \mathcal{E}^i, \tag{3.1.7b}$$

$$u_h \cdot n = \bar{u}_h \cdot n \quad \forall e \in \mathcal{E}^\partial, \tag{3.1.7c}$$

where, for an interior facet e shared by two elements K^- and K^+, $v^\pm$ denotes the trace over $\partial K^\pm$ of a function v.

The HDG scheme (3.1.6) has been analyzed in [13] for the case of a homogeneous Dirichlet boundary value problem. In our context, we have mixed boundary conditions with nonhomogeneous Dirichlet part. Then, to adapt the results provided in [13], we will make a change of variable. Let $\boldsymbol{z} := \boldsymbol{u}_h - \boldsymbol{\varphi}$, with $\boldsymbol{\varphi} := (0, \bar{\varphi})$ and

$$\bar{\varphi} := \begin{cases} \overline{\Pi}_V u_D & , \Gamma_D \\ 0 & , \partial\Omega \backslash \Gamma_D \end{cases}.$$

Then, (3.1.6) is equivalent: Find $(\boldsymbol{z}, \boldsymbol{p}_h) \in \boldsymbol{V}_h^0 \times \boldsymbol{Q}_h$ such that:

$$a_h^{ns}(\boldsymbol{z}, \boldsymbol{v}_h) + o_h^{ns}(z_h; \boldsymbol{z}, \boldsymbol{v}_h) + b_h^{ns}(\boldsymbol{p}_h, \boldsymbol{v}_h) = F(\boldsymbol{v}_h) \qquad \forall \boldsymbol{v}_h \in \boldsymbol{V}_h^0, \tag{3.1.8a}$$

$$b_h^{ns}(\boldsymbol{q}_h, \boldsymbol{u}_h) = 0 \qquad \forall \boldsymbol{q}_h \in \boldsymbol{Q}_h. \tag{3.1.8b}$$

where $F(\boldsymbol{v}_h) = L_h^{ns}(\boldsymbol{v}_h) - a_h^{ns}(\boldsymbol{\varphi}, \boldsymbol{v}_h) - o_h^{ns}(z; \boldsymbol{\varphi}, \boldsymbol{v}_h)$.

Notice that $o_h^{ns}(u_h; \boldsymbol{\varphi}, \boldsymbol{v}_h) = \langle u_h \cdot n\bar{\varphi}, v_h\rangle_{\Gamma_{\text{in}}} = \langle u_h \cdot n\, \overline{\Pi}_V u_D, v_h\rangle_{\Gamma_{\text{in}}} = \langle \overline{\Pi}_V u_D \cdot n\, \overline{\Pi}_V u_D, v_h\rangle_{\Gamma_{\text{in}}}$, thanks to (3.1.7c), and

$$a_h^{ns}(\boldsymbol{\varphi}, \boldsymbol{v}_h) = \langle 2\nu\alpha h_K^{-1}\overline{\Pi}_V u_D, v - \bar{v}\rangle_{\Gamma_D} + \langle 2\nu\overline{\Pi}_V u_D, \varepsilon(v)\cdot n\rangle_{\Gamma_D} - \langle 2\nu\varepsilon(\overline{\Pi}_V u_D)\cdot n, v - \bar{v}\rangle_{\Gamma_D}.$$

3.2 Well-posedness.

The following result states the consistency of the HDG scheme (3.1.6). It can be deduced from the arguments in [13] and [14].

Lemma 3.2.1 (Consistency)**.** *Let* $H^1_{u_D} := \{v \in [H^1(\Omega)]^2 : \gamma(v)|_{\Gamma_D} = u_D\}$*. If* $(u, p) \in [H^1_{u_D}(\Omega)]^2 \cap [H^2(\Omega)]^2 \times L^2_0(\Omega) \cap H^1(\Omega)$ *is solution to* (3.0.1)*, then*

$$a_h^{ns}(\boldsymbol{u}, \boldsymbol{v}_h) + o_h^{ns}(u; \boldsymbol{u}, \boldsymbol{v}_h) + b_h^{ns}(\boldsymbol{p}, \boldsymbol{v}_h) = L_h^{ns}(\boldsymbol{v}_h) \qquad \forall \boldsymbol{v}_h \in \boldsymbol{V}_h^0, \tag{3.2.1a}$$

$$b_h^{ns}(\boldsymbol{q}_h, \boldsymbol{u}) = 0 \qquad \forall \boldsymbol{q} \in \boldsymbol{Q}_h, \tag{3.2.1b}$$

where $\boldsymbol{u} = (u, \gamma(u))$ *and* $\boldsymbol{p} = (p, \gamma(p))$*.*

We now present stability and boundedness results that can be deduced from [13]. We define the spaces

$$V(h) := V_h + [H^1_{\Gamma_D}(\Omega)]^2 \cap [H^2(\Omega)]^2, \qquad Q(h) := Q_h + L^2_0(\Omega) \cap H^1(\Omega)$$
$$\bar{V}(h) := \bar{V}_h^0 + [H^{3/2}_{\Gamma_D}(\partial\mathcal{T})]^2, \qquad \bar{Q}(h) := \bar{Q}_h + H_0^{1/2}(\partial\mathcal{T}),$$

where $H^1_{\Gamma_D}(\Omega)$ is the space of $H^1(\Omega)$-functions with zero trace on Γ_D, $H^{3/2}_{\Gamma_D}(\partial\mathcal{T}_h)$ is the trace space of $H^1_{\Gamma_D}(\Omega) \cap H^2(\Omega)$ and $H_0^{1/2}(\partial\mathcal{T})$ is the trace space of $L^2_0(\Omega) \cap H^1(\Omega)$. Let $\boldsymbol{V}^\star(h) := V(h) \times \bar{V}(h)$, $\boldsymbol{Q}^\star(h) := Q(h) \times \bar{Q}(h)$ and $\boldsymbol{X}^\star(h) := \boldsymbol{V}^\star(h) \times \boldsymbol{Q}^\star(h)$. Frequent use will also be made of functions in the following space:

$$\boldsymbol{V}_h^{\text{div}} := \{\boldsymbol{v}_h \in \boldsymbol{V}_h : b_h^{ns}(\boldsymbol{q}_h, \boldsymbol{v}_h) = 0 \quad \forall \boldsymbol{q}_h \in \boldsymbol{Q}_h\}.$$

We introduce the following mesh-dependent inner-products and norms:

$$(\boldsymbol{u},\boldsymbol{v})_s := (\varepsilon(u),\varepsilon(v))_{\mathcal{T}} + \sum_{K\in\mathcal{T}} h_K^{-1}\langle \bar{u}-u,\bar{v}-v\rangle_{\partial K} \qquad \boldsymbol{u},\boldsymbol{v}\in \boldsymbol{V}^\star(h), \tag{3.2.2a}$$

$$|\!|\!|\boldsymbol{v}|\!|\!|_s := \sum_{K\in\mathcal{T}} \|\varepsilon(v)\|_K^2 + \sum_{K\in\mathcal{T}} h_K^{-1}\|\bar{v}-v\|_{\partial K}^2 \qquad \boldsymbol{v}\in \boldsymbol{V}^\star(h), \tag{3.2.2b}$$

$$|\!|\!|\boldsymbol{v}|\!|\!|_{s'}^2 := |\!|\!|\boldsymbol{v}|\!|\!|_s^2 + \sum_{K\in\mathcal{T}} h_K \left\|\frac{\partial v}{\partial n}\right\|_{\partial K}^2 \qquad \boldsymbol{v}\in \boldsymbol{V}^\star(h), \tag{3.2.2c}$$

$$|\!|\!|\boldsymbol{q}|\!|\!|_p^2 := \|q\|^2 + \sum_{K\in\mathcal{T}} h_K\|\bar{q}\|_{\partial K}^2 \qquad \boldsymbol{q}\in \boldsymbol{Q}^\star(h), \tag{3.2.2d}$$

where we note that $|\!|\!|\cdot|\!|\!|_s$ and $|\!|\!|\cdot|\!|\!|_{s'}$ are equivalent in $\boldsymbol{V}_h^0$, thanks to the discrete trace inequality. We also define

$$|\!|\!|(\boldsymbol{v},\boldsymbol{q})|\!|\!|_{s,p}^2 := \nu|\!|\!|\boldsymbol{v}|\!|\!|_s^2 + \nu^{-1}|\!|\!|\boldsymbol{q}|\!|\!|_p^2 \qquad (\boldsymbol{v},\boldsymbol{q})\in \boldsymbol{X}^\star(h),$$

$$|\!|\!|(\boldsymbol{v},\boldsymbol{q})|\!|\!|_{s',p'}^2 := |\!|\!|(\boldsymbol{v},\boldsymbol{q})|\!|\!|_{s,p}^2 + \sum_{K\in\mathcal{T}} \nu h_K \left\|\frac{\partial v}{\partial n}\right\|_{\partial K}^2 = \nu|\!|\!|\boldsymbol{v}|\!|\!|_{s'}^2 + \nu^{-1}|\!|\!|\boldsymbol{q}|\!|\!|_p^2 \qquad (\boldsymbol{v},\boldsymbol{q})\in \boldsymbol{X}^\star(h).$$

The standard discrete H^1-norm for $v\in V(h)$ is defined as $\|v\|_{1,h} := |\!|\!|(v,\{v\})|\!|\!|_s$, where $\{v\} := \frac{1}{2}(v^+ + v^-)$ is the average operator, and $v^\pm$ denotes the trace of v from the interior of $K^\pm$. Furthermore, we will make use of the following discrete Poincaré inequality:

$$\|v_h\|_{\mathcal{T}} \le c_p\|v_h\|_{1,h} \le c_p|\!|\!|\boldsymbol{v}_h|\!|\!|_s \qquad \forall \boldsymbol{v}_h\in \boldsymbol{V}_h^0, \tag{3.2.3}$$

where c_p is a constant independent of h_K [7, Theorem 5.3]. In addition, according to [12, Theorem 4.4], there exists $c_{tr}>0$, independent of the meshsize, such that

$$\|v_h\|_{0,r,\Gamma_D} \le c_{tr}|\!|\!|\boldsymbol{v}|\!|\!|_s \quad \forall \boldsymbol{v}_h\in \boldsymbol{V}_h^0 \tag{3.2.4}$$

and $r\ge 2$. Also, for $e\in\mathcal{E}$,there exists $c_{eq}>0$, independent of h, such that

$$\|v_h\|_{0,4,e} \le c_{eq}\|h_e^{-1/4}v\|_{0,2,e} \quad \forall v_k\in P_k(e). \tag{3.2.5}$$

For a sufficiently large stabilization parameter α, it was shown [15, Lemmas 4.2 and 4.3] that the bilinear form $a_h^{ns}(\cdot,\cdot)$ is coercive and bounded, i.e., there exist constants $c_a^s > 0$ and $c_a^b > 0$ independent of h such that for all $\boldsymbol{v}_h \in \boldsymbol{V}_h^0$ and $\boldsymbol{u} \in \boldsymbol{V}^\star(h)$

$$a_h^{ns}(\boldsymbol{v}_h, \boldsymbol{v}_h) \geq \nu c_a^s \|\boldsymbol{v}_h\|_s^2 \quad \text{and} \quad |a_h^{ns}(\boldsymbol{u}, \boldsymbol{v}_h)| \leq \nu c_a^b \|\boldsymbol{u}\|_{s'} \|\boldsymbol{v}_h\|_s. \tag{3.2.6}$$

The bilinear form $b_h^{ns}(\cdot,\cdot)$ is also bounded [15, Lemma 4.8], that is, there exists a constant $c_b^b > 0$, independent of h, such that for all $\boldsymbol{q}_h \in \boldsymbol{Q}_h$ and $\boldsymbol{v} \in \boldsymbol{V}^*(h)$,

$$|b_h^{ns}(\boldsymbol{q}_h, \boldsymbol{v})| \leq c_b^b \|\boldsymbol{v}\|_{s'} \|\boldsymbol{q}_h\|_p, \tag{3.2.7}$$

while the following inf-sup condition was proven in [17, Lemma 1]. There exists a constant $\beta_p > 0$, independent of h, such that for all $\boldsymbol{q}_h \in \boldsymbol{Q}_h^\star$

$$\beta_p \|\boldsymbol{q}_h\|_p \leq \sup_{\boldsymbol{v}_h \in \boldsymbol{V}_h^\star} \frac{b_h^{ns}(\boldsymbol{q}_h, \boldsymbol{v}_h)}{\|\boldsymbol{v}_h\|_s}.$$

Therefore, (3.2.6) and (3.2.7) imply the following discrete inf-sup condition. There exists a constant $C^s > 0$, independent of h ν, such that for all, $(\boldsymbol{v}_h, \boldsymbol{q}_h) \in \boldsymbol{V}_h^\star \times \boldsymbol{Q}_h^\star$

$$C^s \|(\boldsymbol{v}_h, \boldsymbol{q}_h)\|_{s,p} \leq \sup_{(\boldsymbol{w}_h, \boldsymbol{r}_h) \in \boldsymbol{V}_h^\star \times \boldsymbol{Q}_h^\star} \frac{a_h^{ns}(\boldsymbol{v}_h, \boldsymbol{w}_h) + b_h^{ns}(\boldsymbol{q}_h, \boldsymbol{w}_h) - b_h^{ns}(\boldsymbol{r}_h, \boldsymbol{v}_h)}{\|(\boldsymbol{w}_h, \boldsymbol{r}_h)\|_{s,p}}. \tag{3.2.8}$$

In addition, by Proposition 3.4 in [4], there exists $M_o^{ns} > 0$ such that, for all $w \in V(h)$, $\boldsymbol{u} \in [H^1(\mathcal{T}_h)]^2 \times [L^2(\mathcal{E})]^2$ and $\boldsymbol{v} \in \boldsymbol{V}_h^0$,

$$o_h^{ns}(w; \boldsymbol{u}, \boldsymbol{v}) \leq M_o^{ns} \|w\|_{1,h} \|\boldsymbol{u}\|_s \|\boldsymbol{v}\|_s. \tag{3.2.9}$$

Moreover, from the proof of Proposition 3.4 in [4], we can deduce that, there exists $M_4^{ns} > 0$ such that, for all $w \in V_h \cap H(\text{div}, \Omega)$, $\boldsymbol{u} \in [H^1(\mathcal{T}_h)]^2 \times [L^2(\mathcal{E})]^2$ and $\boldsymbol{v} \in \boldsymbol{V}_h^0$,

$$o_h^{ns}(w; \boldsymbol{u}, \boldsymbol{v}) \leq M_4^{ns} \|w\|_{0,4,\Omega} \|\boldsymbol{u}\|_s \|\boldsymbol{v}\|_s. \tag{3.2.10}$$

The following identity will also be useful. Let $w \in H(\text{div},\Omega)$ and $\boldsymbol{v} \in [H^1(\mathcal{T})]^2 \times [L^2(\mathcal{E})]^2$. It holds

$$o_h^{ns}(w;\boldsymbol{v},\boldsymbol{v}) = -\frac{1}{2}\langle w\cdot n\,\bar{v},\bar{v}\rangle_{\partial\Omega} + \frac{1}{2}\langle |w\cdot n|\,(v-\bar{v}),(v-\bar{v})\rangle_{\partial\mathcal{T}} + \langle |w\cdot n|\bar{v},\bar{v}\rangle_{\Gamma_{\text{out}}} \tag{3.2.11}$$

and its proof follows from [4, Proposition 3.5].

Theorem 3.2.2. *Let* $C(f,u_D) := \|f\|_\Omega + \nu c_a^s\|h^{-1/2}\overline{\Pi}_V u_D\|_{\Gamma_D} + c_{tr}\|\overline{\Pi}_V u_D\|^2_{0,4,\Gamma_D}$*. The HDG scheme (3.1.8) has at least one solution* $\boldsymbol{u}_h$ *and satisfies*

$$|\!|\!|\boldsymbol{u}_h|\!|\!|_s \le d_{ns}C(f,u_D), \tag{3.2.12}$$

with $d_{ns} > 0$*, independent of* h*. Moreover, if*

$$C(f,u_D) \le \frac{(\nu c_a^s)^2}{c_0^s c_p},$$

then the solution is unique.

Proof. Let $\boldsymbol{v}_h \in \boldsymbol{V}_h^0$. By (3.2.6), We have that

$$\begin{aligned}\|F(\boldsymbol{v}_h)\|_{\mathcal{T}} \le& \|f(\boldsymbol{v}_h)\|_{\mathcal{T}} + \nu c_a^s|\!|\!|\boldsymbol{\varphi}|\!|\!|_s|\!|\!|\boldsymbol{v}_h|\!|\!|_s + |\langle\overline{\Pi}_V u_D\cdot n\,\overline{\Pi}_V u_D, v_h\rangle_{\Gamma_D}|\\ \le& \|f\|_\Omega\|\boldsymbol{v}_h\|_{\mathcal{T}} + \nu c_a^s|\!|\!|\boldsymbol{\varphi}|\!|\!|_s|\!|\!|\boldsymbol{v}_h|\!|\!|_s + \|\overline{\Pi}_V u_D\|^2_{0,4,\Gamma_D}\|v_h\|_{0,2,\Gamma_D}\\ \le& \|f\|_\Omega\|\boldsymbol{v}_h\|_{\mathcal{T}} + \nu c_a^s|\!|\!|\boldsymbol{\varphi}|\!|\!|_s|\!|\!|\boldsymbol{v}_h|\!|\!|_s + c_{tr}\|\overline{\Pi}_V u_D\|^2_{0,4,\Gamma_D}|\!|\!|\boldsymbol{v}_h|\!|\!|_s,\end{aligned}$$

where we have used (3.2.4). Since $|\!|\!|\boldsymbol{\varphi}|\!|\!|_s = \|h^{-1/2}\overline{\Pi}_V u_D\|_{\Gamma_D}$, we obtain

$$\|F\|_{\mathcal{T}} \le \|f\|_\Omega + \nu c_a^s\|h^{-1/2}\overline{\Pi}_V u_D\|_{\Gamma_D} + c_{tr}\|\overline{\Pi}_V u_D\|^2_{0,4,\Gamma_D} =: C(f,u_D).$$

Since $C(f,u_D) \le \frac{(\nu c_a^s)^2}{c_0^s c_p}$, by following the same steps of the proof of Lemma 1 in [13] adapted to our context, we can deduce that (3.1.8) has a solution and satisfies

$$|\!|\!|\boldsymbol{z}|\!|\!|_s \le \frac{c_p}{\nu c_a^s}C(f,u_D).$$

The estimate in (3.2.12) follows after noticing that $\|\boldsymbol{u}_h\|_s \leq \|\boldsymbol{z}\|_s + \|\boldsymbol{\varphi}\|_s$ and setting $d_{ns} := \dfrac{c_p}{\nu c_a^s} + 1$.

Finally, assuming $C(f, u_D) \leq \frac{(\nu c_a^s)^2}{c_0^s c_p}$, from the same steps of the proof of Lemma 1 in [13] we can deduce uniqueness. □

CHAPTER 4

The Coupled Problem.

Taking into account the HDG schemes in Sections 3.1.2 and 2.1, the HDG scheme to discretize (1.0.1) reads: Find $(\boldsymbol{u}_h, \boldsymbol{p}_h) \in \boldsymbol{V}_h^{g_{\phi_h}} \times \boldsymbol{Q}_h$ and $\boldsymbol{\phi}_h \in \boldsymbol{C}_h^{\phi_{\text{in}}}$ such that:

$$a_h^{ns}(\boldsymbol{u}_h, \boldsymbol{v}_h) + o_h^{ns}(u_h; \boldsymbol{u}_h, \boldsymbol{v}_h) + b_h^{ns}(\boldsymbol{p}_h, \boldsymbol{v}_h) = L_h^{ns}(\boldsymbol{v}_h) \qquad \forall \boldsymbol{v}_h \in \boldsymbol{V}_h^0, \tag{4.0.1a}$$

$$b_h^{ns}(\boldsymbol{q}_h, \boldsymbol{u}_h) = 0 \qquad \forall \boldsymbol{q}_h \in \boldsymbol{Q}_h, \tag{4.0.1b}$$

$$o_h^c(u_h; \boldsymbol{\phi}_h, \boldsymbol{r}_h) + a_h^c(\boldsymbol{\phi}_h, \boldsymbol{r}_h) + \langle c_2 \bar{\phi}_h, \bar{r}_h \rangle_\Sigma = 0. \qquad \forall \boldsymbol{r}_h \in \boldsymbol{C}_h^0, \tag{4.0.1c}$$

where, for the Navier-Stokes part, $\Gamma_D = \Gamma_{\text{in}} \cup \Sigma$ and

$$g_{\phi_h} = \begin{cases} (c_0 - c_1 \bar{\phi}_h) n & \text{on } \Sigma, \\ u_{\text{in}} & \text{on } \Gamma_{\text{in}}. \end{cases} \tag{4.0.1d}$$

Remark 2. We observe in (1.0.1) that $f = 0$, but we will keep it to cover the case of non-zero sources.

The following result is a consequence of Lemmas 3.2.1 and 2.1.1

Lemma 4.0.1 (Consistency)**.** *Let* $(u,p) \in [H^1_{g_\phi}(\Omega)]^2 \cap [H^2(\Omega)]^2 \times L^2_0(\Omega) \cap H^1(\Omega)$ *and* $\phi \in H^2(\Omega)$ *solution of* (1.0.1a)*. We have*

$$a_h^{ns}(\boldsymbol{u}, \boldsymbol{v}_h) + o_h^{ns}(u; \boldsymbol{u}, \boldsymbol{v}_h) + b_h^{ns}(\boldsymbol{p}, \boldsymbol{v}_h) = L_h^{ns}(\boldsymbol{v}_h) \qquad \forall \boldsymbol{v}_h \in \boldsymbol{V}_h^0, \tag{4.0.2a}$$

$$b_h^{ns}(\boldsymbol{q}_h, \boldsymbol{u}) = 0 \qquad \forall \boldsymbol{q}_h \in \boldsymbol{Q}_h, \tag{4.0.2b}$$

$$o_h^c(u; \boldsymbol{\phi}, \boldsymbol{r}_h) + a_h^c(\boldsymbol{\phi}, \boldsymbol{r}_h) + \langle c_2 \gamma(\phi), \bar{r}_h \rangle_\Sigma = 0. \qquad \forall \boldsymbol{r}_h \in \boldsymbol{C}_h^0, \tag{4.0.2c}$$

where $\boldsymbol{u} = (u, \gamma(u))$*,* $\boldsymbol{p} = (p, \gamma(p))$*,* $\boldsymbol{\phi} = (\phi, \gamma(\phi))$ *and we recall that*

$$H^1_{g_\phi}(\Omega) := \{v \in H^1(\Omega) : \gamma(v)|_{\Gamma_D} = g_\phi\}.$$

To analyze the well-posedness of the HDG scheme (4.0.1), we will use a fixed-point strategy. To that end, we define the following operators associated with the Navier-Stokes and advection-diffusion solvers. More precisely, let

$$\begin{aligned} S : \bar{C}_h^{\phi_{\text{in}}} &\longrightarrow \boldsymbol{V}_h^{\text{div}} \\ \bar{\mu} &\longmapsto S(\bar{\mu}) = \boldsymbol{u}^\mu, \end{aligned}$$

where $\boldsymbol{V}_h^{\text{div}} := \{\boldsymbol{v}_h \in \boldsymbol{V}_h : b_h^{ns}(\boldsymbol{q}_h, \boldsymbol{v}_h) = 0\,, \forall \boldsymbol{q}_h \in Q_h\}$ and $\boldsymbol{u}^\mu$ is such that $(\boldsymbol{u}^\mu, \boldsymbol{p}^\mu) \in \boldsymbol{V}_h^{g_\mu} \times \boldsymbol{Q}_h$ is the only solution (Theorem 3.2.2) to

$$a_h^{ns}(\boldsymbol{u}^\mu, \boldsymbol{v}_h) + o_h^{ns}(u^\mu; \boldsymbol{u}^\mu, \boldsymbol{v}_h) + b_h^{ns}(\boldsymbol{p}^\mu, \boldsymbol{v}_h) = L_h^{ns}(\boldsymbol{v}_h) \qquad \forall \boldsymbol{v}_h \in \boldsymbol{V}_h^0, \tag{4.0.3a}$$

$$b_h^{ns}(\boldsymbol{q}_h, \boldsymbol{u}^\mu) = 0 \qquad \forall \boldsymbol{q}_h \in \boldsymbol{Q}_h, \tag{4.0.3b}$$

where we recall that the Dirichlet data is given by

$$g_\mu = \begin{cases} (c_0 - c_1 \bar{\mu}) n & \text{on } \Sigma, \\ u_{\text{in}} & \text{on } \Gamma_{\text{in}}. \end{cases}$$

In addition, let

$$T: \boldsymbol{V}_h^{\text{div}} \longrightarrow \bar{C}_h^{\phi_{\text{in}}}$$
$$\boldsymbol{w} \longmapsto T(\boldsymbol{w}) = \bar{\mu}^w,$$

where $\bar{\mu}^w$ is such that $\boldsymbol{\mu}^w = (\mu^w, \bar{\bar{\mu}}^w) \in \boldsymbol{C}_h^{\phi_{\text{in}}}$ is the solution to

$$o_h^c(w; \boldsymbol{\mu}^w, \boldsymbol{r}_h) + a_h^c(\boldsymbol{\mu}^w, \boldsymbol{r}_h) + \langle c_2 \bar{\mu}^w, \bar{r}_h \rangle_\Sigma = 0, \tag{4.0.4}$$

for all $\boldsymbol{r}_h \in \boldsymbol{C}_h^0$. According to Theorem 2.2.3, if $\|\gamma_n(w)\|_\Sigma \leq 2R$, this problem is well-posed. In addition,

$$\|\boldsymbol{\mu}\|_D \leq C_T \|\phi_{\text{in}}(c_2 - \gamma_n(w))\|_\Sigma,$$

and

$$\|\bar{\mu}\|_\Sigma \leq \widehat{C}_T \|\phi_{\text{in}}(c_2 - \gamma_n(w))\|_\Sigma + \|\phi_{\text{in}}\|_\Sigma. \tag{4.0.5}$$

Showing well-posedness of the HDG scheme (4.0.1), is equivalent to finding a fixed-point of the following operator:

$$\boldsymbol{J}: \boldsymbol{C}_h^{\phi_{\text{in}}} \longrightarrow \boldsymbol{C}_h^{\phi_{\text{in}}}$$
$$\boldsymbol{\mu} \longmapsto \boldsymbol{J}(\boldsymbol{\mu}) = (\mu, (T \circ S)\bar{\mu}).$$

Let us define the convex set $\boldsymbol{B} := \{\boldsymbol{\mu} \in \boldsymbol{C}_h^{\phi_{\text{in}}} : \; c_1^{1/2} \|\bar{\mu}\|_\Sigma \leq R\}$ where $R = \dfrac{C_a^t}{4c_{st}}$. We recall that $C_a^t > 0$ and c_{st} are the constants defined in Lemma 2.2.2.

Lemma 4.0.2. *Let us assume the following conditions on the given coefficients c_0, c_1 and c_2, and the given inlet concentration ϕ_{in}:*

$$c_1^{1/2} \phi_{\text{in}} \widehat{C}_T \leq \frac{1}{4} R, \quad c_1^{1/2} c_2 \phi_{\text{in}} \widehat{C}_T |\Sigma| \leq \frac{1}{4} R, \quad c_0 |\Sigma| \leq R, \quad c_1 \leq 1,$$

$$c_0\phi_{\text{in}}|\Sigma|\widehat{C}_T \leq \frac{1}{4}R, \quad c_1^{1/2}\phi_{\text{in}}\widehat{C}_T \qquad \leq\frac{1}{4} \quad , \quad c_1^{1/2}\phi_{\text{in}}|\Sigma|\leq\frac{1}{4}R,$$

where we recall that $\widehat{C}_T$ is the constant defined in Theorem 2.2.3. Then $\boldsymbol{J}(\boldsymbol{B}) \subset \boldsymbol{B}$.

Remark 3. In practice, the above assumptions are satisfied since c_0, c_1 and c_2 are small, as we can deduce from Table 6.5.

Proof. Let $\boldsymbol{\mu} \in \boldsymbol{B}$, $\boldsymbol{u}^\mu := S(\bar{\mu})$ and $\bar{\varphi} := (T \circ S)\bar{\mu} = T(\boldsymbol{u}^\mu)$. We have

$$\|u^\mu \cdot n\|_\Sigma = \|(c_0 - c_1\bar{\mu})n\|_\Sigma \leq c_0|\Sigma| + c_1\|\bar{\mu}\|_\Sigma \leq 2R = \frac{C_a^t}{2c_{st}}, \tag{4.0.6}$$

since $c_1^{1/2} \leq c_1$. Then, by Theorem 2.2.3,

$$\begin{aligned} c_1^{1/2}\|(T \circ S)(\bar{\mu})\|_\Sigma =& c_1^{1/2}\|\bar{\varphi}\|_\Sigma \leq c_1^{1/2}\widehat{C}_T\|\phi_{\text{in}}(c_2 - \gamma_n(u^\mu))\|_\Sigma + c_1^{1/2}\|\phi_{\text{in}}\|_\Sigma \\ \leq& c_1^{1/2}\widehat{C}_T\phi_{\text{in}}c_2|\Sigma| + c_1^{1/2}\phi_{\text{in}}\widehat{C}_T\|u^\mu \cdot n\|_\Sigma + c_1^{1/2}\phi_{\text{in}}|\Sigma| \\ \leq& \frac{1}{2}R + \frac{1}{4}\|u^\mu \cdot n\|_\Sigma. \end{aligned}$$

Hence, by (4.0.6), $c_1^{1/2}\|(T \circ S)(\bar{\mu})\|_\Sigma \leq R$, i.e., $\boldsymbol{J}(\boldsymbol{B}) \subset \boldsymbol{B}$. □

Lemma 4.0.3. *If there exists a positive constant M_{c_1}, independent of h and c_1, such that $(c_1 h_e^{-1})^{1/2} \leq M_{c_1}$ for all $e \subset \Sigma$, then $\boldsymbol{J} : \boldsymbol{B} \to \boldsymbol{B}$ is a continuous operator, i.e, there exists $L_J > 0$, independent of h, such that.*

$$\|J(\boldsymbol{\mu}_1) - J(\boldsymbol{\mu}_2)\|_D \leq L_J\|\boldsymbol{\mu}_1 - \boldsymbol{\mu}_2\|_D \quad \forall \boldsymbol{\mu}_1, \boldsymbol{\mu}_2 \in \boldsymbol{B},$$

Remark 4. The assumption $(c_1 h_e^{-1})^{1/2} \leq M_{c_1}$ for all $e \subset \Sigma$ is very strong. This is due to the continuous dependence result (3.2.12) and the presence of non-homogeneous Dirichlet boundary conditions. In practice, c_1 is of the order of $10^{-8} m^4/(\text{mol}\, s)$ (see Table 6.5).

Proof. Let $\boldsymbol{\mu}_1, \boldsymbol{\mu}_2 \in \boldsymbol{B}$. We set $\boldsymbol{u}_i := S(\boldsymbol{\mu}_i)$ and $\boldsymbol{\varphi}_i := T(\boldsymbol{u}_i) = J(\boldsymbol{\mu}_i)$, for $i \in \{1, 2\}$. By (2.1.4), we have

$$o_h^c(u_i; \boldsymbol{\varphi}_i, \boldsymbol{r}_h) + a_h^c(\boldsymbol{\varphi}_i, \boldsymbol{r}_h) + \langle c_2\bar{\varphi}_i, \bar{r}_h\rangle_\Sigma = 0 \qquad \forall \boldsymbol{r}_h \in \boldsymbol{C}_h^0 \quad \forall i \in \{1, 2\}.$$

Adding over $i \in \{1,2\}$, this implies that

$$o_h^c(u_1; \boldsymbol{\varphi}_1, \boldsymbol{r}_h) - o_h^c(u_2; \boldsymbol{\varphi}_2, \boldsymbol{r}_h) + a_h^c(\boldsymbol{\varphi}, \boldsymbol{r}_h) + \langle c_2 \bar{\varphi}, \bar{r}_h \rangle_\Sigma = 0 \qquad \forall \boldsymbol{r}_h \in \boldsymbol{C}_h^0,$$

with $\boldsymbol{\varphi} := \boldsymbol{\varphi}_1 - \boldsymbol{\varphi}_2 \in \boldsymbol{C}_h^0$. Then, rearranging terms,

$$o_h^c(u_1; \boldsymbol{\varphi}_1, \boldsymbol{r}_h) - o_h^c(u_2; \boldsymbol{\varphi}_1, \boldsymbol{r}_h) + o_h^c(u_2; \boldsymbol{\varphi}, \boldsymbol{r}_h) + a_h^c(\boldsymbol{\varphi}, \boldsymbol{r}_h) + \langle c_2 \bar{\varphi}, \bar{r}_h \rangle_\Sigma = 0, \qquad \forall \boldsymbol{r}_h \in \boldsymbol{C}_h^0.$$

Since $\boldsymbol{\varphi} \in \boldsymbol{C}_h^0$, we can take $\boldsymbol{r}_h = \boldsymbol{\varphi}$ and obtain

$$o_h^c(u_1; \boldsymbol{\varphi}_1, \boldsymbol{\varphi}) - o_h^c(u_2; \boldsymbol{\varphi}_1, \boldsymbol{\varphi}) + o_h^c(u_2; \boldsymbol{\varphi}, \boldsymbol{\varphi}) + a_h^c(\boldsymbol{\varphi}, \boldsymbol{\varphi}) + \langle c_2 \bar{\varphi}, \bar{\varphi} \rangle_\Sigma = 0.$$

By (2.2.5a) and (2.2.5b), we deduce that

$$\begin{aligned} C_a^t \|\boldsymbol{\varphi}\|_D^2 + c_2 \|\bar{\varphi}\|_\Sigma^2 \leq & - o_h^c(u_1; \boldsymbol{\varphi}_1, \boldsymbol{\varphi}) + o_h^c(u_2; \boldsymbol{\varphi}_1, \boldsymbol{\varphi}) - o_h^c(u_2; \boldsymbol{\varphi}, \boldsymbol{\varphi}) \\ = & o_h^c(u_2 - u_1; \boldsymbol{\varphi}_1, \boldsymbol{\varphi}) - \frac{1}{2} \| |u_2 \cdot n|^{1/2} (\varphi - \bar{\varphi}) \|_{\partial \mathcal{T}}^2 + \frac{1}{2} \langle u_2 \cdot n, \bar{r}^2 \rangle_\Sigma - \frac{1}{2} \langle u_2 \cdot n, \bar{r}^2 \rangle_{\Gamma_{\text{out}}} \\ \leq & o_h^c(u_2 - u_1; \boldsymbol{\varphi}_1, \boldsymbol{\varphi}) + \frac{1}{2} \langle u_2 \cdot n, \bar{\varphi}^2 \rangle_\Sigma . \end{aligned}$$

Now, by the same arguments that led to (2.2.7), we can deduce that

$$\frac{1}{2} \langle u_2 \cdot n, \bar{\varphi}^2 \rangle_\Sigma \leq c_{sc} \|u_2 \cdot n\|_\Sigma \, \|\boldsymbol{\varphi}\|_D^2 .$$

Therefore,

$$\left(C_a^t - c_{sc} \|u_2 \cdot n\|_\Sigma \right) \|\boldsymbol{\varphi}\|_D^2 \leq o_h^c(u_2 - u_1; \boldsymbol{\varphi}_1, \boldsymbol{\varphi}) \leq M_o \|u_1 - u_2\|_{1,h} \|\boldsymbol{\varphi}_1\|_D \|\boldsymbol{\varphi}\|_D .$$

where we have used (2.2.4d). Since $\boldsymbol{u}_1 - \boldsymbol{u}_2$ vanishes on Γ_{in}, by the discrete Poincaré inequality [7, Theorem 5.4], there exists $c_p > 0$ such that $\|u_1 - u_2\|_{1,h} \leq c_p \|\boldsymbol{u}_1 - \boldsymbol{u}_2\|_s$. Thus,

$$\left(C_a^t - c_{sc} \|u_2 \cdot n\|_\Sigma \right) \|\boldsymbol{\varphi}\|_D \leq M_o \|\boldsymbol{u}_1 - \boldsymbol{u}_2\|_s \|\boldsymbol{\varphi}_1\|_D . \tag{4.0.7}$$

Now, according to(3.2.12),

$$\|\boldsymbol{u}_1 - \boldsymbol{u}_2\|_s \leq d_{ns} C(0, g_\mu).$$

with

$$g_\mu = \begin{cases} -c_1 \bar{\mu} n & \text{on } \Sigma, \\ 0 & \text{on } \Gamma_{\text{in}}, \end{cases} \tag{4.0.8}$$

$\bar{\mu} := \bar{\mu}_1 - \bar{\mu}_2$ and

$$C(0, g_\mu) = \nu c_a^s c_1 \|h^{-1/2} \bar{\mu}\|_\Sigma + c_{tr} c_1 \|\bar{\mu}\|_{0,4,\Sigma}^2.$$

Replacing this expression in (4.0.7),

$$\left(C_a^t - c_{sc}\|u_2 \cdot n\|_\Sigma\right) \|\boldsymbol{\varphi}\|_D \leq M_o d_{ns} C(0, g_\mu) \|\boldsymbol{\varphi}_1\|_D. \tag{4.0.9}$$

Since, for $i \in \{1, 2\}$, $\boldsymbol{\mu}_i \in \boldsymbol{B}$, by (4.0.6) we have $\|u^i \cdot n\|_\Sigma \leq C_a^t/(2c_{st}) = 2R$ and, by Theorem 2.2.3, we know that

$$\begin{aligned} \|\boldsymbol{\varphi}_1\|_D \leq & C_T \|\phi_{\text{in}}(c_2 - \gamma_n(u_1))\|_\Sigma = C_T \|\phi_{\text{in}}(c_2 - c_0 + c_0 \bar{\mu})\|_\Sigma \\ \leq & C_T \phi_{\text{in}} |c_2 - c_0||\Sigma| + C_T c_1 \phi_{\text{in}} \|\bar{\mu}\|_\Sigma \\ \leq & C_T \phi_{\text{in}} |c_2 - c_0||\Sigma| + C_T c_1^{1/2} \phi_{\text{in}} R, \end{aligned} \tag{4.0.10}$$

and (4.0.9) implies

$$\frac{C_a^t}{2} \|\boldsymbol{\varphi}\|_D \leq M_o C_T d_{ns} C(0, g_\mu)\, \phi_{\text{in}} \left(|c_2 - c_0||\Sigma| + c_1^{1/2} R\right). \tag{4.0.11}$$

Now, by (3.2.5) and the assumption that $(c_1 h_e^{-1})^{1/2} \leq M_{c_1}$ for all $e \subset \Sigma$, then

$$C(0, g_\mu) \leq \nu c_a^s c_1 \|h^{-1/2} \bar{\mu}\|_\Sigma + c_{tr} c_1 c_{eq}^2 \|h^{-1/4} \bar{\mu}\|_\Sigma^2$$

$$\leq \nu c_a^s c_1^{1/2} M_{c_1} \|\bar{\mu}\|_\Sigma + c_{tr} c_1^{1/2} M_{c_1} c_{eq}^2 \|\bar{\mu}\|_\Sigma^2$$
$$\leq \left(\nu c_a^s M_{c_1} c_{tr} + c_{tr}^2 c_1^{1/2} M_{c_1} c_{eq}^2 \|\bar{\mu}\|_\Sigma\right) \|\boldsymbol{\mu}\|_D.$$

where we have used (2.2.3). Since $\boldsymbol{\mu} \in \boldsymbol{B}$, then $c_1^{1/2} \|\bar{\mu}\|_\Sigma \leq R$. Therefore,

$$C(0, g_\mu) \leq \left(\nu c_a^s M_{c_1} c_{tr} + c_{tr}^2 M_{c_1} c_{eq}^2 R\right) \|\boldsymbol{\mu}\|_D.$$

Thus, replacing this expression in (4.0.11), we obtain

$$\frac{C_a^t}{2} \|\boldsymbol{\varphi}\|_D \leq M_o C_T d_{ns} \left(\nu c_a^s M_{c_1} c_{tr} + c_{tr}^2 M_{c_1} c_{eq}^2 R\right) \phi_{\text{in}} \left(|c_2 - c_0||\Sigma| + c_1^{1/2} R\right) \|\boldsymbol{\mu}\|_D. \qquad (4.0.12)$$

This implies the result with

$$L_J := \frac{2}{C_a^t} M_o C_T d_{ns} \left(\nu c_a^s M_{c_1} c_{tr} + c_{tr}^2 M_{c_1} c_{eq}^2 R\right) \phi_{\text{in}} \left(|c_2 - c_0||\Sigma| + c_1^{1/2} R\right). \qquad (4.0.13)$$

□

Corollary 4.0.1. *If c_1 are sufficiently small, then $\boldsymbol{J}$ has a fixed point. Moreover, if c_0, c_1 and c_2 are small enough, then $\boldsymbol{J}$ is a contraction and therefore has a unique fixed point.*

Proof. Existence follows from Brouwer fixed-point theorem and Lemmas 4.0.2 and 4.0.3. In addition, f c_0, c_1 and c_2 are small enough, then $L_J < 1$ and therefore $\boldsymbol{J}$ has a unique fixed-point.

□

CHAPTER 5

Error analysis.

Let $(\boldsymbol{u}, p) \in [H^1_{g_\phi}(\Omega)]^2 \times L^2_0(\Omega)$ and $\phi \in H^1_{\phi_{\text{in}}}(\Omega)$ the solution to (1.1.1), and $(\boldsymbol{u}_h, \boldsymbol{p}_h) \in \boldsymbol{V}_h^{g_{\phi_h}} \times \boldsymbol{Q}_h$ and $\boldsymbol{\phi}_h \in \boldsymbol{C}_h^{\phi_{\text{in}}}$ the solution to (4.0.1). We introduce the interpolation errors

$$
\begin{aligned}
I_\phi &:= \phi - \Pi_C \phi \qquad & I_{\bar{\phi}} &:= \gamma(\phi) - \overline{\Pi}_C \gamma(\phi) \\
I_u &:= u - \Pi_{BDM} u \qquad & I_{\bar{u}} &:= \gamma(u) - \overline{\Pi}_V \gamma(u),
\end{aligned}
$$

where $\Pi_{BDM} : [H^1(\Omega)]^d \to V_h$ be the usual Brezzi-Douglas-Marini (BDM) interpolation operator (see, for example, [13, Lemma 2]) and Π_C is the standard L^2-projection onto C_h. We recall that $\overline{\Pi}_V$ and $\overline{\Pi}$ are the L^2-projection over $\bar{V}_h$ and $\bar{C}_h$, resp. We set $\boldsymbol{I}_\phi := (I_\phi, I_{\bar{\phi}})$ and $\boldsymbol{I}_u := (I_u, I_{\bar{u}})$.

The approximation errors are defined as follows.

$$
\begin{aligned}
\varepsilon_\phi &:= \Pi_C \phi - \phi_h, \qquad & \varepsilon_{\bar{\phi}} &:= \overline{\Pi}_C \gamma(\phi) - \bar{\phi}_h, \\
\varepsilon_u &:= \Pi_{BDM} u - u_h, \qquad & \varepsilon_{\bar{u}} &:= \overline{\Pi}_V u - \bar{u}_h.
\end{aligned}
$$

We define $\boldsymbol{\varepsilon_\phi} := (\varepsilon_\phi, \varepsilon_{\bar{\phi}})$ and $\boldsymbol{\varepsilon_u} := (\varepsilon_u, \varepsilon_{\bar{u}})$.

For convenience, we also write $\boldsymbol{\phi} := (\phi, \gamma(\phi))$ and $\boldsymbol{u} := (u\gamma(u))$. In this way, we can decompose the errors as

$$\boldsymbol{\phi} - \boldsymbol{\phi}_h = \boldsymbol{\varepsilon_\phi} + \boldsymbol{I_\phi} \quad \text{and} \quad \boldsymbol{u} - \boldsymbol{u}_h = \boldsymbol{\varepsilon_u} + \boldsymbol{I_u}.$$

Now, by (4.0.1) and consistency (4.0.2a), we have

$$a_h^{ns}(\boldsymbol{u} - \boldsymbol{u}_h, \boldsymbol{v}_h) + o_h^{ns}(u; \boldsymbol{u}, \boldsymbol{v}_h) - o_h^{ns}(u_h; \boldsymbol{u}_h, \boldsymbol{v}_h) + b_h^{ns}(\boldsymbol{p} - \boldsymbol{p}_h, \boldsymbol{v}_h) = 0 \quad \forall \boldsymbol{v}_h \in \boldsymbol{V}_h^0, \quad (5.0.1a)$$

$$b_h^{ns}(\boldsymbol{q}_h, \boldsymbol{u} - \boldsymbol{u}_h) = 0 \quad \forall \boldsymbol{q}_h \in \boldsymbol{Q}_h, \quad (5.0.1b)$$

$$o_h^c(u; \boldsymbol{\phi}, \boldsymbol{r}_h) - o_h^c(u_h; \boldsymbol{\phi}_h, \boldsymbol{r}_h) + a_h^c(\boldsymbol{\phi} - \boldsymbol{\phi}_h, \boldsymbol{r}_h) + \langle c_2\gamma(\phi) - \bar{\phi}_h, \bar{r}_h \rangle_\Sigma = 0. \quad \forall \boldsymbol{r}_h \in \boldsymbol{C}_h^0. \quad (5.0.1c)$$

We now proceed with the error bound for the approximation error associated with the concentration. As we will see, the first error bound depends on the approximation error of the velocity.

Lemma 5.0.1. *Let $C_c := C_T \phi_{\text{in}} |c_2 - c_0||\Sigma| + C_T c_1^{1/2} \phi_{\text{in}} R$. It holds*

$$\left(C_a^t - \frac{1}{2} c_{sc} \| |u \cdot n|^{1/2} \|_\Sigma \right) \| \boldsymbol{\varepsilon_\phi} \|_D \leq \ (M_a + M_o \|u\|_{1,h}) \| \boldsymbol{I_\phi} \|_{D'} + c_2\, c_{sc} \| I_{\bar{\phi}} \|_\Sigma$$
$$+ C_c M_o (c_p \| \boldsymbol{\varepsilon_u} \|_s + \| I_u \|_{1,h}).$$

Proof. Since $\varepsilon_\phi \in \boldsymbol{C}_h^0$, by (2.2.5b) and using (5.0.1c), we deduce that

$$C_a^t \| \boldsymbol{\varepsilon_\phi} \|_D^2 \leq a_h^c(\boldsymbol{\varepsilon_\phi}, \boldsymbol{\varepsilon_\phi}) = -\, a_h^c(\boldsymbol{I_\phi}, \boldsymbol{\varepsilon_\phi}) + a_h^c(\boldsymbol{\phi} - \boldsymbol{\phi}_h, \boldsymbol{\varepsilon_\phi})$$
$$= -\, a_h^c(\boldsymbol{I_\phi}, \boldsymbol{\varepsilon_\phi}) - c_2 \langle \gamma(\phi) - \bar{\phi}_h, \varepsilon_{\bar{\phi}} \rangle_\Sigma + T,$$

where $T := -o_h^c(u; \boldsymbol{\phi}, \boldsymbol{\varepsilon_\phi}) + o_h^c(u_h; \boldsymbol{\phi}_h, \boldsymbol{\varepsilon_\phi})$. We can decompose T as

$$T = -o_h^c(u, \boldsymbol{\varepsilon_\phi}, \boldsymbol{\varepsilon_\phi}) - o_h^c(\varepsilon_u; \boldsymbol{\phi}_h, \boldsymbol{\varepsilon_\phi}) - o_h^c(u; \boldsymbol{I_\phi}, \boldsymbol{\varepsilon_\phi}) - o_h^c(I_u; \boldsymbol{\phi}_h, \boldsymbol{\varepsilon_\phi})$$

and by (2.2.5a),

$$
\begin{aligned}
T = &-\frac{1}{2}\||\gamma_n(u)|^{1/2}(\varepsilon_\phi - \varepsilon_{\bar{\phi}})\|^2_{\partial\mathcal{T}} + \frac{1}{2}\langle\gamma_n(u), \varepsilon^2_{\bar{\phi}}\rangle_\Sigma - \frac{1}{2}\langle\gamma_n(u), \varepsilon^2_{\bar{\phi}}\rangle_{\Gamma_{\rm out}} \\
&- o^c_h(\varepsilon_u; \boldsymbol{\phi}_h, \boldsymbol{\varepsilon}_{\boldsymbol{\phi}}) - o^c_h(u; \boldsymbol{I}_{\boldsymbol{\phi}}, \boldsymbol{\varepsilon}_{\boldsymbol{\phi}}) - o^c_h(I_u; \boldsymbol{\phi}_h, \boldsymbol{\varepsilon}_{\boldsymbol{\phi}}) \\
\le\ & \frac{1}{2}\langle\gamma_n(u), \varepsilon^2_{\bar{\phi}}\rangle_\Sigma - o^c_h(\varepsilon_u; \boldsymbol{\phi}_h, \boldsymbol{\varepsilon}_{\boldsymbol{\phi}}) - o^c_h(u; \boldsymbol{I}_{\boldsymbol{\phi}}, \boldsymbol{\varepsilon}_{\boldsymbol{\phi}}) - o^c_h(I_u; \boldsymbol{\phi}_h, \boldsymbol{\varepsilon}_{\boldsymbol{\phi}}).
\end{aligned}
$$

Now, by (2.2.4d),

$$
\begin{aligned}
T \le\ & \frac{1}{2}\langle\gamma_n(u), \varepsilon^2_{\bar{\phi}}\rangle_\Sigma + M_o\|\varepsilon_u\|_{1,h}\|\boldsymbol{\phi}_h\|_D\|\boldsymbol{\varepsilon}_{\boldsymbol{\phi}}\|_D \\
&+ M_o\|u\|_{1,h}\|\boldsymbol{I}_{\boldsymbol{\phi}}\|_{D'}\|\boldsymbol{\varepsilon}_{\boldsymbol{\phi}}\|_D + M_o\|I_u\|_{1,h}\|\boldsymbol{\phi}_h\|_D\|\boldsymbol{\varepsilon}_{\boldsymbol{\phi}}\|_D.
\end{aligned}
$$

Thus,

$$
\begin{aligned}
C^t_a\|\boldsymbol{\varepsilon}_{\boldsymbol{\phi}}\|^2_D \le\ & a^c_h(\boldsymbol{I}_{\boldsymbol{\phi}}, \boldsymbol{\varepsilon}_{\boldsymbol{\phi}}) - c_2\langle\gamma(\phi) - \bar{\phi}_h, \varepsilon_{\bar{\phi}}\rangle_\Sigma + \frac{1}{2}\langle\gamma_n(w), \varepsilon^2_{\bar{\phi}}\rangle_\Sigma + M_o\|\varepsilon_u\|_{1,h}\|\boldsymbol{\phi}_h\|_D\|\boldsymbol{\varepsilon}_{\boldsymbol{\phi}}\|_D \\
&+ M_o\|u\|_{1,h}\|\boldsymbol{I}_{\boldsymbol{\phi}}\|_{D'}\|\boldsymbol{\varepsilon}_{\boldsymbol{\phi}}\|_D + M_o\|I_u\|_{1,h}\|\boldsymbol{\phi}_h\|_D\|\boldsymbol{\varepsilon}_{\boldsymbol{\phi}}\|_D \\
\le\ & M_a\|\boldsymbol{I}_{\boldsymbol{\phi}}\|_{D'}\|\boldsymbol{\varepsilon}_{\boldsymbol{\phi}}\|_D - c_2\langle I_{\bar{\phi}} + \varepsilon_{\bar{\phi}}, \varepsilon_{\bar{\phi}}\rangle_\Sigma + \frac{1}{2}\langle\gamma_n(u), \varepsilon^2_{\bar{\phi}}\rangle_\Sigma + M_o\|\varepsilon_u\|_{1,h}\|\boldsymbol{\phi}_h\|_D\|\boldsymbol{\varepsilon}_{\boldsymbol{\phi}}\|_D \\
&+ M_o\|u\|_{1,h}\|\boldsymbol{I}_{\boldsymbol{\phi}}\|_{D'}\|\boldsymbol{\varepsilon}_{\boldsymbol{\phi}}\|_D + M_o\|I_u\|_{1,h}\|\boldsymbol{\phi}_h\|_D\|\boldsymbol{\varepsilon}_{\boldsymbol{\phi}}\|_D,
\end{aligned}
$$

where we have used (2.2.4b).

Now, we observe that

$$
-c_2\langle I_{\bar{\phi}} + \varepsilon_{\bar{\phi}}, \varepsilon_{\bar{\phi}}\rangle_\Sigma \le -c_2\langle I_{\bar{\phi}}, \varepsilon_{\bar{\phi}}\rangle_\Sigma \le c_2\, c_{sc}\|I_{\bar{\phi}}\|_\Sigma\|\boldsymbol{\varepsilon}_{\boldsymbol{\phi}}\|_D,
$$

by the same arguments used to prove (2.2.7). Similarly, we have

$$
\frac{1}{2}\langle\gamma_n(u), \varepsilon^2_{\bar{\phi}}\rangle_\Sigma \le \frac{1}{2}c_{sc}\||u\cdot n|^{1/2}\|_\Sigma\, \|\boldsymbol{\varepsilon}_{\boldsymbol{\phi}}\|_D.
$$

Therefore,

$$
\left(C^t_a - \frac{1}{2}c_{sc}\||u\cdot n|^{1/2}\|_\Sigma\right)\|\boldsymbol{\varepsilon}_{\boldsymbol{\phi}}\|^2_D \le\ M_a\|\boldsymbol{I}_{\boldsymbol{\phi}}\|_{D'}\|\boldsymbol{\varepsilon}_{\boldsymbol{\phi}}\|_D + c_2\, c_{sc}\|I_{\bar{\phi}}\|_\Sigma\|\boldsymbol{\varepsilon}_{\boldsymbol{\phi}}\|_D + M_o\|\varepsilon_u\|_{1,h}\|\boldsymbol{\phi}_h\|_D\|\boldsymbol{\varepsilon}_{\boldsymbol{\phi}}\|_D
$$

$$+ M_o\|u\|_{1,h}\|\boldsymbol{I}_\phi\|_{D'}\|\boldsymbol{\varepsilon_\phi}\|_D + M_o\|I_u\|_{1,h}\|\boldsymbol{\phi}_h\|_D\|\boldsymbol{\varepsilon_\phi}\|_D.$$

Since the Poincaré inequality (3.2.3) is also valid for functions that vanish in part of the boundary, $\|\boldsymbol{\varepsilon}_u\|_{1,h} \leq c_p\|\boldsymbol{\varepsilon}_u\|_s$, we have

$$\left(C_a^t - \frac{1}{2}c_{sc}\||u\cdot n|^{1/2}\|_\Sigma\right)\|\boldsymbol{\varepsilon_\phi}\|_D \leq \;(M_a + M_o\|u\|_{1,h})\|\boldsymbol{I_\phi}\|_{D'} + c_2\, c_{sc}\|I_{\bar{\phi}}\|_\Sigma$$
$$+ M_o(c_p\|\boldsymbol{\varepsilon_u}\|_s + \|I_u\|_{1,h})\|\boldsymbol{\phi}_h\|_D.$$

Finally, by the same arguments that led to (4.0.10), we obtain

$$\|\boldsymbol{\phi}_h\|_D \leq C_T\phi_{\text{in}}|c_2 - c_0||\Sigma| + C_T c_1^{1/2}\phi_{\text{in}}R := C_c, \tag{5.0.2}$$

and the result follows. □

On the other hand, to bound the approximation error of the velocity, from (5.0.1a) with $\boldsymbol{v}_h = \boldsymbol{\varepsilon}_u$,

$$a_h^{ns}(\boldsymbol{u}-\boldsymbol{u}_h, \boldsymbol{\varepsilon_u}) + o_h^{ns}(u;\boldsymbol{u},\boldsymbol{\varepsilon}_u) - o_h^{ns}(u_h;\boldsymbol{u}_h,\boldsymbol{\varepsilon_u}) + b_h^{ns}(\boldsymbol{p}-\boldsymbol{p}_h,\boldsymbol{\varepsilon_u}) = 0.$$

By the properties of the BDM projection (cf. [13, Lemma 2])and using that u_h is pointwise divergence-free and divergence-conforming (3.1.7), we observe that $b_h^{ns}(\boldsymbol{p}-\boldsymbol{p}_h,\boldsymbol{\varepsilon_u}) = 0$. Then, after rearranging terms and using the error decomposition, we have

$$a_h^{ns}(\boldsymbol{\varepsilon_u},\boldsymbol{\varepsilon_u}) = -a_h^{ns}(\boldsymbol{\varepsilon_u},\boldsymbol{I_u}) - o_h^{ns}(u;\boldsymbol{\varepsilon_u},\boldsymbol{\varepsilon_u}) - o_h^{ns}(\varepsilon_u;,\boldsymbol{u}_h,\boldsymbol{\varepsilon_u}) - o_h^{ns}(u;\boldsymbol{I}_u,\boldsymbol{\varepsilon_u}) - o_h^{ns}(I_u,\boldsymbol{u}_h,\boldsymbol{\varepsilon_u}).$$

Then, by coercivity of a_h^{ns} (3.2.6), we obtain

$$\nu c_a^s\|\boldsymbol{\varepsilon}_u\|_s^2 \leq -\, a_h^{ns}(\boldsymbol{I_u},\boldsymbol{\varepsilon_u}) - o_h^{ns}(u;\boldsymbol{\varepsilon_u},\boldsymbol{\varepsilon_u}) - o_h^{ns}(\varepsilon_u;\boldsymbol{u}_h,\boldsymbol{\varepsilon_u})$$
$$- o_h^{ns}(u;\boldsymbol{I_u},\boldsymbol{\varepsilon_u}) - o_h^{ns}(I_u;\boldsymbol{u}_h,\boldsymbol{\varepsilon_u}).$$

Furthermore, by (3.2.11),

$$o_h^{ns}(u;\boldsymbol{\varepsilon_u},\boldsymbol{\varepsilon_u}) \geq -\frac{1}{2}\langle (u\cdot n)\varepsilon_{\bar{u}},\varepsilon_{\bar{u}}\rangle_\Sigma + \frac{1}{2}\langle (u\cdot n)\varepsilon_{\bar{u}},\varepsilon_{\bar{u}}\rangle_{\Gamma_{\text{out}}} \geq -\frac{1}{2}\langle (u\cdot n)\varepsilon_{\bar{u}},\varepsilon_{\bar{u}}\rangle_\Sigma.$$

Then,

$$\begin{aligned}
\nu c_a^s \|\boldsymbol{\varepsilon_u}\|_s^2 \leq& - a_h^{ns}(\boldsymbol{I_u},\boldsymbol{\varepsilon_u}) + \frac{1}{2}\langle (u\cdot n)\varepsilon_{\bar{u}},\varepsilon_{\bar{u}}\rangle_\Sigma \\
&- o_h^{ns}(\varepsilon_u;\boldsymbol{u}_h,\boldsymbol{\varepsilon_u}) - o_h^{ns}(u;\boldsymbol{I_u},\boldsymbol{\varepsilon_u}) - o_h^{ns}(I_u;\boldsymbol{u}_h,\boldsymbol{\varepsilon_u}) \\
\leq& \nu c_a^b \|\boldsymbol{I}_u\|_{s'}\|\boldsymbol{\varepsilon}_u\|_s + 2(c_{sc,1}^2 + c_{sc,2}^2)\|u\cdot n\|_\Sigma \|\boldsymbol{\varepsilon}_u\|_s^2 \\
&- o_h^{ns}(\varepsilon_u;\boldsymbol{u}_h,\boldsymbol{\varepsilon_u}) - o_h^{ns}(u;\boldsymbol{I_u},\boldsymbol{\varepsilon_u}) - o_h^{ns}(I_u;\boldsymbol{u}_h,\boldsymbol{\varepsilon_u}),
\end{aligned} \tag{5.0.3}$$

where we used (3.2.6) and the same arguments that led to (2.2.7). We next bound each of the last three terms in the right-hand side separately. For the first, since ε_u vanishes on Γ_{in}, by (3.2.9) we have

$$o_h^{ns}(\varepsilon_u;\boldsymbol{u}_h,\boldsymbol{\varepsilon_u}) \leq M_o^{ns}\|\boldsymbol{\varepsilon}_u\|_{1,h}\|\boldsymbol{u}_h\|_s\|\boldsymbol{\varepsilon_u}\|_s. \tag{5.0.4}$$

For the second term, by (3.2.10), we obtain

$$o_h^{ns}(u;\boldsymbol{I_u},\boldsymbol{\varepsilon_u}) \leq M_4^{ns}\|u\|_{0,4,\Omega}\|\boldsymbol{I_u}\|_s\|\boldsymbol{\varepsilon_u}\|_s. \tag{5.0.5}$$

Now, for the last term,

$$o_h^{ns}(I_u;\boldsymbol{u}_h,\boldsymbol{\varepsilon_u}) \leq M_4^{ns}\|I_u\|_{0,4,\Omega}\|\boldsymbol{u}_h\|_s\|\boldsymbol{\varepsilon_u}\|_s. \tag{5.0.6}$$

Finally, after combining (5.0.3)-(5.0.6), we conclude that

$$\begin{aligned}
(\nu c_a^s - \|u\cdot n\|_\Sigma)\|\boldsymbol{\varepsilon_u}\|_s \leq& \nu c_a^b \|\boldsymbol{I}_u\|_{s'} + M_o^{ns}\|\boldsymbol{\varepsilon}_u\|_{1,h}\|\boldsymbol{u}_h\|_s \\
&+ M_4^{ns}\|u\|_{0,4,\Omega}\|\boldsymbol{I_u}\|_s + M_4^{ns}\|I_u\|_{0,4,\Omega}\|\boldsymbol{u}_h\|_s\|\boldsymbol{\varepsilon_u}\|_s.
\end{aligned}$$

Now, the Poincaré inequality (3.2.3) is also valid for functions that vanish in part of the boundary, then $\|\boldsymbol{\varepsilon}_u\|_{1,h} \le c_p |\!|\!| \boldsymbol{\varepsilon}_u |\!|\!|_s$. Thus,

$$\nu c_a^s |\!|\!| \boldsymbol{\varepsilon}_{\boldsymbol{u}} |\!|\!|_s \ \le \nu c_a^b |\!|\!| \boldsymbol{I}_u |\!|\!|_{s'} + M_o^{ns} c_p |\!|\!| \boldsymbol{\varepsilon}_{\boldsymbol{u}} |\!|\!|_s |\!|\!| \boldsymbol{u}_h |\!|\!|_s + M_4^{ns} \|u\|_{L^4(\Omega)} |\!|\!| \boldsymbol{I}_{\boldsymbol{u}} |\!|\!|_s + M_4^{ns} \|I_u\|_{0,4,\Omega} |\!|\!| \boldsymbol{u}_h |\!|\!|_s.$$

In other words, we have proved the following result.

Lemma 5.0.2. *There holds*

$$\left(\nu c_a^s - \|u \cdot n\|_\Sigma - M_o^{ns} c_p |\!|\!| \boldsymbol{u}_h |\!|\!|_s\right) |\!|\!| \boldsymbol{\varepsilon}_{\boldsymbol{u}} |\!|\!|_s \ \le \nu c_a^b |\!|\!| \boldsymbol{I}_u |\!|\!|_{s'} + M_4^{ns} \|u\|_{L^4(\Omega)} |\!|\!| \boldsymbol{I}_{\boldsymbol{u}} |\!|\!|_s + M_4^{ns} \|I_u\|_{0,4,\Omega} |\!|\!| \boldsymbol{u}_h |\!|\!|_s.$$

Combining Corollaries 5.0.1 and 5.0.2, we obtain the following estimates.

Corollary 5.0.1. *If*

$$\|u \cdot n\|_\Sigma + M_o^{ns} c_p |\!|\!| \boldsymbol{u}_h |\!|\!|_s \le \nu c_a^s / 2 \tag{5.0.7}$$

and $\| |u \cdot n|^{1/2} \|_\Sigma \le C_a^t / s_{sc}$, *we have*

$$|\!|\!| \boldsymbol{\varepsilon}_{\boldsymbol{u}} |\!|\!|_s \ \lesssim |\!|\!| \boldsymbol{I}_{\boldsymbol{u}} |\!|\!|_{s'} + \|u\|_{L^4(\Omega)} |\!|\!| \boldsymbol{I}_{\boldsymbol{u}} |\!|\!|_s + M_4^{ns} \|I_u\|_{0,4,\Omega}.$$

and

$$|\!|\!| \boldsymbol{\varepsilon}_{\boldsymbol{\phi}} |\!|\!|_D \lesssim \ (1 + M\|u\|_{1,h}) |\!|\!| \boldsymbol{I}_{\boldsymbol{\phi}} |\!|\!|_{D'} + c_2 \|I_{\bar{\phi}}\|_\Sigma + C_c(|\!|\!| \boldsymbol{\varepsilon}_{\boldsymbol{u}} |\!|\!|_s + \|I_u\|_{1,h}).$$

Remark 5. Unfortunately, we were unable to prove (5.0.7). Now, according to Remark 1, $u \cdot n$ is small in practice. On the other hand, from (3.2.12),

$$\begin{aligned} |\!|\!| \boldsymbol{u}_h |\!|\!|_s \le & d_{ns} \Bigg(\|f\|_\Omega + \nu c_a^s \|h^{-1/2} u_{\text{in}}\|_{\Gamma_{\text{in}}} + \nu c_a^s \|h^{-1/2}(c_0 - c_1 \phi)\|_\Sigma \\ & + c_{tr} \|u_{\text{in}}\|_{0,4,\Gamma_{\text{in}}}^2 + c_{tr} \|c_0 - c_1 \phi\|_{0,4,\Sigma}^2 \Bigg). \end{aligned}$$

In other words, due to the non-homogeneous boundary condition, the continuous dependence result (3.2.12) provides a negative power of h accompanying the functions at the boundary, and this is why we were unable to show a uniform bound for $\|\boldsymbol{u}_h\|_s$. How to obtain a more convenient continuous dependence result is the subject of ongoing work.

Proposition 5.0.1. Let us assume that $u \in [H^{k+1}(\Omega)]^2$ and $\phi \in H^{k+1}(\Omega)$. There hold

$$
\begin{aligned}
\|\boldsymbol{I_u}\|_{s'} &\lesssim h^k |u|_{k+1,\Omega},\\
\|\boldsymbol{I}_\phi\|_{D'} &\lesssim h^k |\phi|_{k+1,\Omega},\\
\|I_u\|_{1,4} &\lesssim h^k |u|_{k+1,\Omega},\\
\|I_u\|_{0,4,\Omega} &\lesssim h^{k+3/2} |u|_{k+1,4,\Omega}.
\end{aligned}
$$

Proof. The first three estimates follow from Lemma 2 in [13] and the properties of the L^2-projection over faces. Now, for the last estimate,

$$
\begin{aligned}
\|I_u\|_{0,4,\Omega}^4 = \sum_{K\in\mathcal{T}} \|I_u\|_{0,4,K}^4 &\lesssim \sum_{K\in\mathcal{T}} h_K^2 \|\widehat{I}_u\|_{0,4,\widehat{K}}^4\\
&\lesssim \sum_{K\in\mathcal{T}} h_K^2 \|\widehat{u}\|_{k+1,4,\widehat{K}}^4\\
&\lesssim \sum_{K\in\mathcal{T}} h_K^2 h_K^{4(k+1)} \|u\|_{k+1,4,K}^4,
\end{aligned}
$$

by an scaling argument, Bramble-Hilbert ([9, Lemma B.68]). Thus, $\|I_u\|_{0,4,\Omega} \lesssim h^{k+3/2}\|u\|_{k+1,4,\Omega}$.

□

Finally, from Corollary 5.0.1 and previous proposition, we conclude the following result

Theorem 5.0.3. *Let us assume that $u \in [H^{k+1}(\Omega)]^2 \cap [W_4^{k+1}(\Omega)]^2$, $p \in H^{k+1}(\Omega)$ and $\phi \in H^{k+1}(\Omega)$. Suppose that the assumption of Corollary 5.0.1 hold. We have that*

$$
\begin{aligned}
\|\boldsymbol{u} - \boldsymbol{u}_h\|_s &\lesssim h^k |u|_{k+1,\Omega} + h^{k+3/2}|u|_{k+1,4,\Omega},\\
\|\boldsymbol{\phi} - \boldsymbol{\phi}_h\|_s &\lesssim h^k |\phi|_{k+1,\Omega},\\
\|p - p_h\| &\lesssim h^k \left(|p|_{k+1,\Omega} + |u|_{k+1,\Omega}\right).
\end{aligned}
$$

CHAPTER 6

Numerical simulations

This chapter is devoted to test the performance of the scheme (4.0.1). we will first consider manufactured solutions to compute the experimental order of convergence, and then simulate real scenarios in desalination channels. We implemented (4.0.1) in NGsolve [18].

The algorithm is based on the fixed-point iteration described in Chapter 4.

Picard's iterarion. Given ϕ and w, we compute $P_\phi(w) := \boldsymbol{u}_h$, where $(\boldsymbol{u}_h, \boldsymbol{p}_h) \in \boldsymbol{V}_h^{g_\phi} \times \boldsymbol{Q}_h$ is such that

$$a_h^{ns}(\boldsymbol{u}_h, \boldsymbol{v}_h) + o_h^{ns}(w; \boldsymbol{u}_h, \boldsymbol{v}_h) + b_h^{ns}(\boldsymbol{p}_h, \boldsymbol{v}_h) = L_h^{ns}(\boldsymbol{v}_h) \qquad \forall \boldsymbol{v}_h \in \boldsymbol{V}_h^0, \tag{6.0.1a}$$

$$b_h^{ns}(\boldsymbol{q}_h, \boldsymbol{u}_h) = 0 \qquad \forall \boldsymbol{q}_h \in \boldsymbol{Q}_h, \tag{6.0.1b}$$

where we recall that the Dirichlet data is given by

$$g_\phi = \begin{cases} (c_0 - c_1\phi)n & \text{on } \Sigma, \\ u_{\text{in}} & \text{on } \Gamma_{\text{in}}. \end{cases}$$

Algorithm 1 Navier-Stokes($\bar{\phi}$,w_0)

Give a concentration $\bar{\phi}$, a velocity w_0 and atolerance tol_{NS}.
Set w_1 =NaN.
$\text{it}_{NS} = 1$
while $tol_{NS} < diff$ **do**
    $\boldsymbol{u}_h = P_\phi(w_0)$, solution to (6.0.1).
    $w_1 = u_h$
    $diff = \|w_1 - w_0\|_\Omega$
    $w_0 = w_1$
    $\text{it}_{NS} = \text{it}_{NS} + 1$
end while
Return $\boldsymbol{u}_h$

Algorithm 2 Fixed-point algorithm

Give the inlet concentration ϕ_{in} and velocity $\boldsymbol{u}_{\text{in}}$.
Give an initial concentration $\bar{\phi}^{(0)}$ and a tolerance *tol*.
$\boldsymbol{\phi}^{(1)}$ =NaN.
$\text{it}_T = 1$
while *tol* <diff **do**
    $\boldsymbol{u}_h$ = Navier-Stokes($\bar{\phi}^{(0)}$, u_{in})
    $\boldsymbol{\phi}^{(1)} = T(\boldsymbol{u}_h)$ the solution to (4.0.4) with inlet boundary condition ϕ_{in}.
    $diff = \|\boldsymbol{\phi}^{(1)} - \boldsymbol{\phi}^{(0)}\|_\Omega$
    $\boldsymbol{\phi}^{(0)} = \boldsymbol{\phi}^{(1)}$
    $\text{it}_T = \text{it}_T + 1$
end while
Return $\boldsymbol{\phi}^{(1)}$

6.1 Manufactured solutions.

In this section, we test our scheme with manufactured solutions. For a variable v, we denote by e_v the errors in L^2-norm associated to v. The experimental rate of convergence is defined as:

$$r_v := \frac{\log(e_v/e'_v)}{\log(h/h')}.$$

where e_v and e'_v are the errors computed by two consecutive meshsizes h and h'.

Example 1. We consider the domain Ω as the unit square with boundaries Γ_{in}, Γ_{out} and Σ as shown in Figure 6.1.

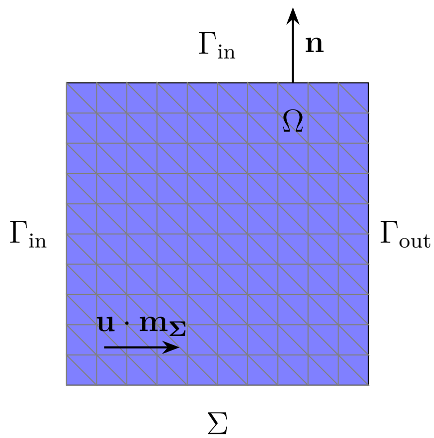

Figure 6.1: Example 1. Domain $\Omega := (0, 1) \times (0, 1)$.

For the numerical test, we consider the exact velocity

$$u(x, y) = \left(y(2 + \cos(2\pi x)\sin(2\pi y)), \frac{-1}{2\pi}\sin(2\pi x)(2\pi y\cos(2\pi y) - \sin(2\pi y)) - 0.1 \right),$$

pressure

$$p(x, y) = \sin(\pi x)\cos(\pi y)$$

and concentration

$$\phi(x, y) = \cos(\pi y)\sin(\pi x).$$

We set

$$c_0 = 0.1 + \sin(\pi x) \quad , \quad c_1 = 1 \quad , \quad c_2 = 0.1 \quad , \quad \theta = 0.1 \quad , \quad \nu = 0.01.$$

Table 6.1 shows the history of convergence for $k = 2$. We observe that the errors in u and ϕ decay with order $k+1$, while the order of convergence of the pressure is k.

h	e_u	r_u	e_p	r_p	e_ϕ	r_ϕ	it$_{NS}$+it$_T$
0.4	$1.0e-01$	-	$7.6e-02$	-	$5.7e-02$	-	24
0.2	$1.1e-02$	3.1	$1.5e-02$	2.3	$2.0e-03$	4.8	22
0.1	$1.1e-03$	3.3	$2.7e-03$	2.4	$1.3e-04$	3.9	22
0.05	$1.2e-04$	3.2	$6.1e-04$	2.1	$1.3e-05$	3.3	21
0.025	$1.5e-05$	3.0	$1.5e-04$	2.0	$1.5e-06$	3.1	23
0.0125	$1.8e-06$	3.0	$3.7e-05$	2.0	$2.4e-07$	2.7	23

Table 6.1: Example 1: Errors and experimental convergence rates, $k = 2$.

In the last column, we display the total number of iterations counting Piccard's iteration of Algorithm 1 and the fixed-point Algorithm 2.

In turn, we can visualize the concentration obtained in Figure 6.2.

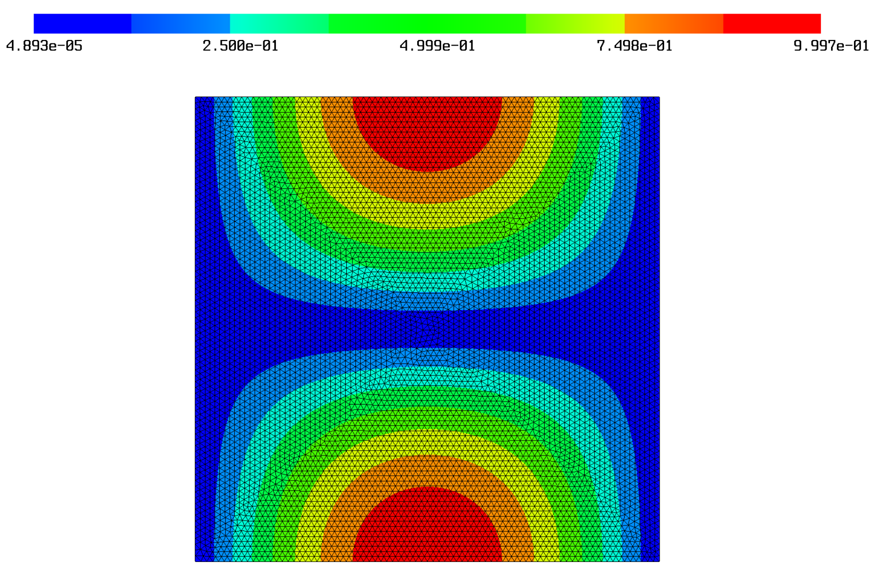

Figure 6.2: Concentration with $h = 0.0125$ and $k = 2$. Example 1.

Example 2. We now consider a case of two membranes. The domain is the square $(0.1, 0.4) \times (0.0, 0.4)$ as shown in Figure 6.3. For the manufactured solution, we consider

$$u(x, y) = \left(y(2 + \cos(2\pi x)\sin(2\pi y)), \frac{-1}{2\pi}\sin(2\pi x)(2\pi y\cos(2\pi y) - \sin(2\pi y)) - 0.1\right),$$

$$p(x, y) = \sin(\pi x)\cos(\pi y)$$

and

$$\phi(x, y) = \cos(\pi y)\sin(\pi x).$$

In Tables 6.2-6.4 we display the history of convergence considering different meshsizes a polinomial degree $k \in \{1, 2, 3\}$. The experimental orders of convergence are $k + 1$ for the velocity and concentration, and k for the pressure.

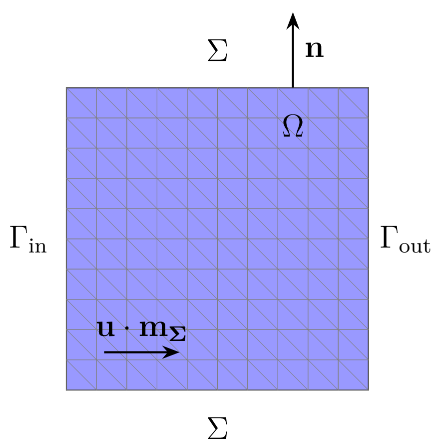

Figure 6.3: Example 2. $\Omega = (0.1, 0.4) \times (0.0, 0.4)$.

h	e_u	r_u	e_p	r_p	e_ϕ	r_ϕ	it$_{NS}$+it$_T$
0.4	$3.4e-02$	-	$9.5e-02$	-	$4.6e-02$	-	37
0.2	$8.1e-03$	2.02	$3.5e-02$	3.7	$8.4e-03$	2.4	31
0.1	$3.3e-03$	1.3	$2.2e-02$	0.66	$2.4e-03$	1.8	24
0.05	$5.7e-04$	2.5	$9.5e-03$	1.2	$4.4e-04$	2.4	26
0.025	$1.3e-04$	2.1	$4.5e-03$	1.07	$1.0e-04$	2.1	22
0.0125	$3.2e-05$	2.0	$2.2e-03$	1.03	$2.5e-05$	2.0	20

Table 6.2: Example 2: Errors and experimental convergence rates, $k = 1$.

h	e_u	r_u	e_p	r_p	e_ϕ	r_ϕ	it$_{NS}$+it$_T$
0.4	$2.2e-02$	-	$2.6e-02$	-	$1.1e-02$	-	26
0.2	$2.6e-03$	2.5	$4.1e-03$	1.3	$1.5e-03$	2.8	25
0.1	$4.1e-04$	2.6	$1.3e-03$	1.6	$2.5e-04$	2.5	23
0.05	$3.4e-05$	3.5	$2.1e-04$	2.6	$8.1e-06$	4.9	19
0.025	$3.7e-06$	3.2	$5.3e-05$	1.9	$7.6e-07$	3.4	18
0.0125	$4.3e-07$	3.1	$1.3e-05$	2.0	$1.2e-07$	2.6	21

Table 6.3: Example 2: Errors and experimental convergence rates, $k = 2$.

h	e_u	r_u	e_p	r_p	e_ϕ	r_ϕ	it$_{NS}$+it$_T$
0.4	$1.0e-02$	-	$7.8e-03$	-	$1.1e-02$	-	28
0.2	$2.1e-04$	5.5	$3.2e-04$	4.6	$5.2e-05$	7.7	25
0.1	$2.8e-05$	2.9	$8.8e-05$	1.8	$4.2e-06$	3.6	24
0.05	$8.3e-07$	5.0	$5.5e-06$	4.0	$9.5e-08$	5.4	18

Table 6.4: Example 2: Errors and experimental convergence rates, $k = 3$.

We can visualize the computed concentration obtained in Figure 6.4:

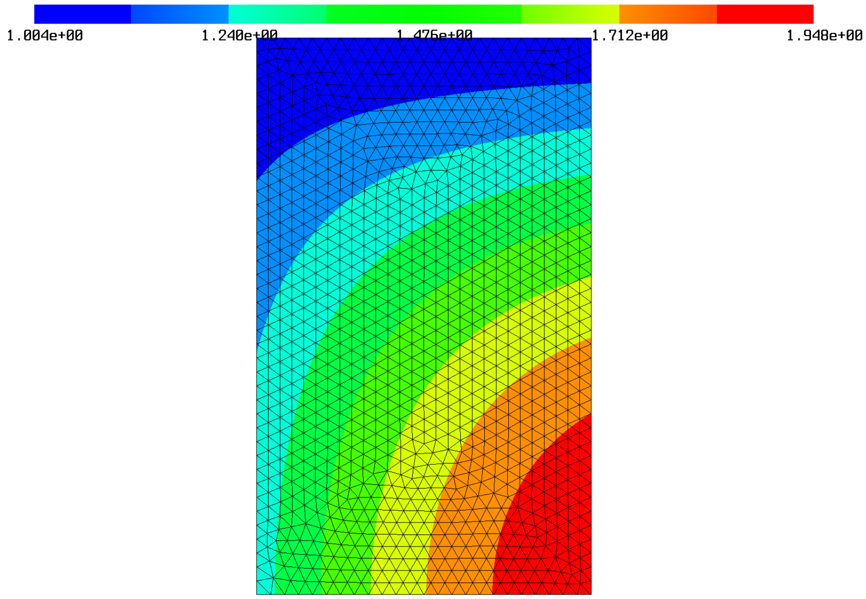

Figure 6.4: Concentration with $h = 0.0125$ and order $k = 3$

6.1.1 Simulations in a desalination channel.

The computational domain associated with a desalination channel is $\Omega = (0, L) \times (0, d)$, where $L = 15mm$ and $d = 0.74mm$. We compared the solution obtained by our scheme with the simulations performed in [1] on a single feed channel. We consider the physical parameters in Table 6.5 [3, 20]. We recall that $c_0 := A\Delta P$, $c_1 := AiRT$ y $c_2 := B$.

Parameter	Meaning	Value	Units
T	System temperature	298	K
R	Ideal gas constant	8.314	$Jmol^{-1}K^{-1}$
i	Number of ions from salt solution	2	$-$
ΔP	Hydrostatic transmembrane pressure	$\Delta P_1 := 4053000$ $\Delta P_2 := 5575875$	Pa
ρ	Feed/permeate fluid density	1027.2	$kg\,m^{-3}$
κ	Feed/permeate diffusivity of salt in water	1.611×10^{-9}	m^2s^{-1}
μ	Feed/permeate fluid dynamic viscosity	8.9×10^{-4}	$kg\,m^{-1}s^{-1}$
A	Membrane water permeability	2.5×10^{-12}	$ms^{-1}\,Pa^{-1}$
B	Membrane salt permeability	2.5×10^{-8}	$m\,s^{-1}$

Table 6.5: global physical parameters

The inlet velocity profile is set as follows.

$$\boldsymbol{u}_{\text{in}} := \left(6u_{\text{in}}\frac{y}{d}\left(1-\frac{y}{d}\right), 2(c_0 - c_1\phi_{\text{in}})\frac{y}{d} - (c_0 - c_1\phi_{\text{in}})\right)^t, \quad y \in [0, d]$$

Simulation 1. A feed channel without salt concentration. We consider a channel without explicit spacers and the numerical method is validated by comparing it with classical analytical models of momentum transport in membrane moduli, i.e., Poiseuille and Berman flow models, by comparing the pressure drop, denoted as $\Delta p := p(0, d/2) - p(x, d/2)$. This validation involves the simulation of a uniform permeation of a pure solvent ($\phi_f = 0$), and then the pressure drop is obtained by solving the equations of motion with the following boundary conditions:

$$\mathbf{u} \cdot \mathbf{n} = c_0 \quad \text{(for Berman flow)} \quad \text{on} \quad \Sigma \quad \text{and} \quad \mathbf{u} \cdot \mathbf{n} = 0 \quad \text{(for Poiseuille flow)} \quad \text{on} \quad \Sigma.$$

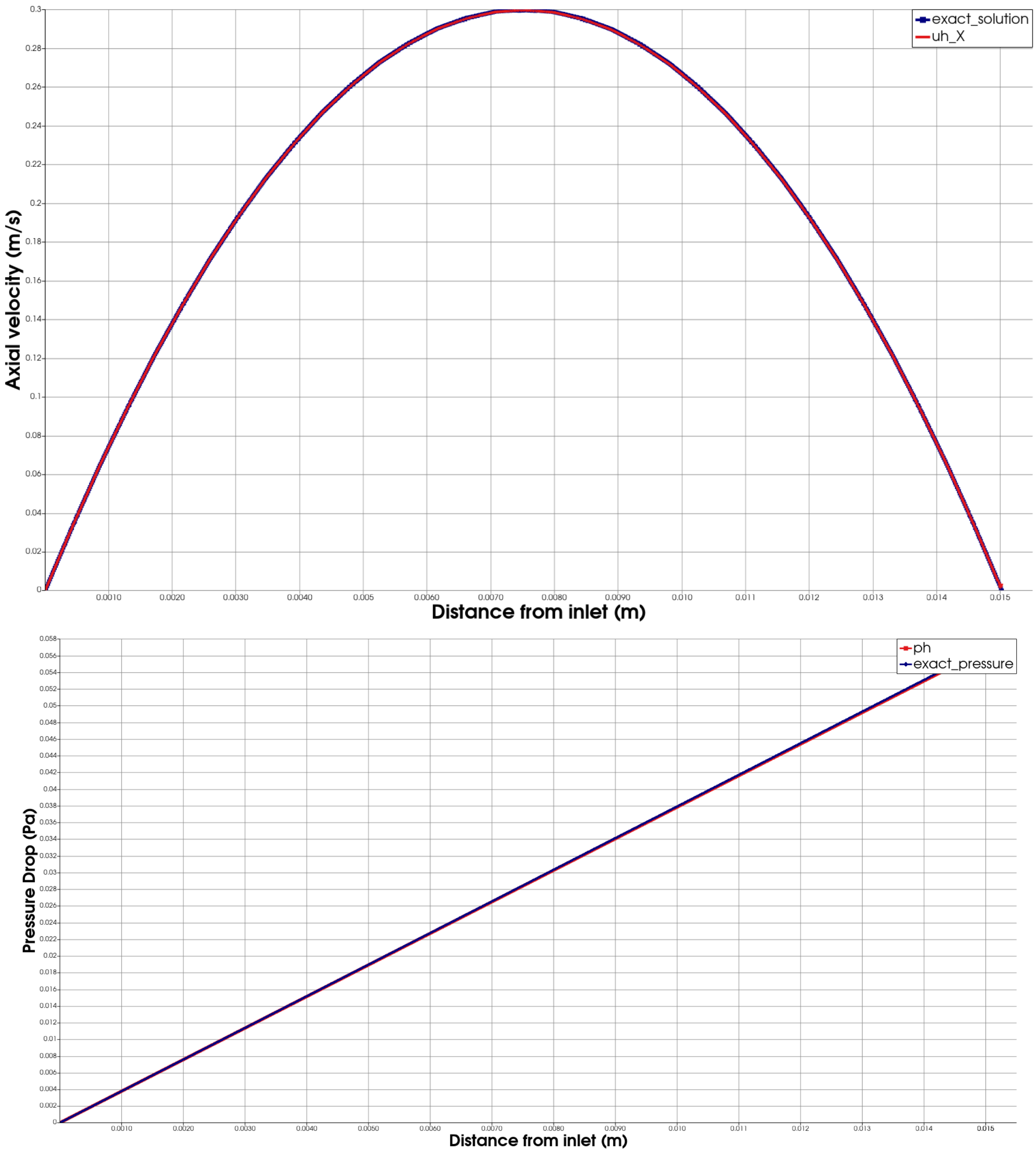

Figure 6.5: Comparison of exact vs. approximate pressure drop (bottom) and axial velocity (top) for a single channel. Simulation conditions: $u_{\text{in}} = 0.2\ m/s$, $\Delta P = \Delta P_2$ and clean water, $h = 4,8e-4$ and $k = 2$

In this case,

$$\Delta p(x, d/2) := \left(\frac{1}{2}\rho u_{\text{in}}^2\right)\left(\frac{24}{Re}\right)\left(\frac{2x}{d}\right),$$

where $Re := \dfrac{2\,\rho\, d\, u_{\rm in}}{\mu}$.

In Figure 6.5 we show the first component of the velocity along $y = d/2$ and the pressure drop. Because there is no salt concentration, the velocity in the entire channel is the same as the inlet velocity. Moreover, since $\boldsymbol{u}_{\rm in}$ is quadratic and we are using $k = 2$, the HDG scheme computes the exact velocity, as we can see in Figure 6.5. Similarly, since Δp is linear, the pressure drop is computed exactly by the scheme as we can observe in Figure 6.5.

Simulation 2. We now consider $u_{\rm in} := 0.1\ m/s$ $\phi_{\rm in} = 600\ mol/m^3$ and $\Delta P = \Delta P_1 = 4053000\ Pa$. In Figure 6.7 we plot the approximation of the concentration. As expected, we observe accumulation of salt along the membranes. To make this clearer, in Figure 6.6 we show the concentration values along the bottom membrane Σ. Starting in $\phi_{\rm in} = 600\ mol$, salt accumulates along the membrane, which also agrees with Figure 3.4 in [1].

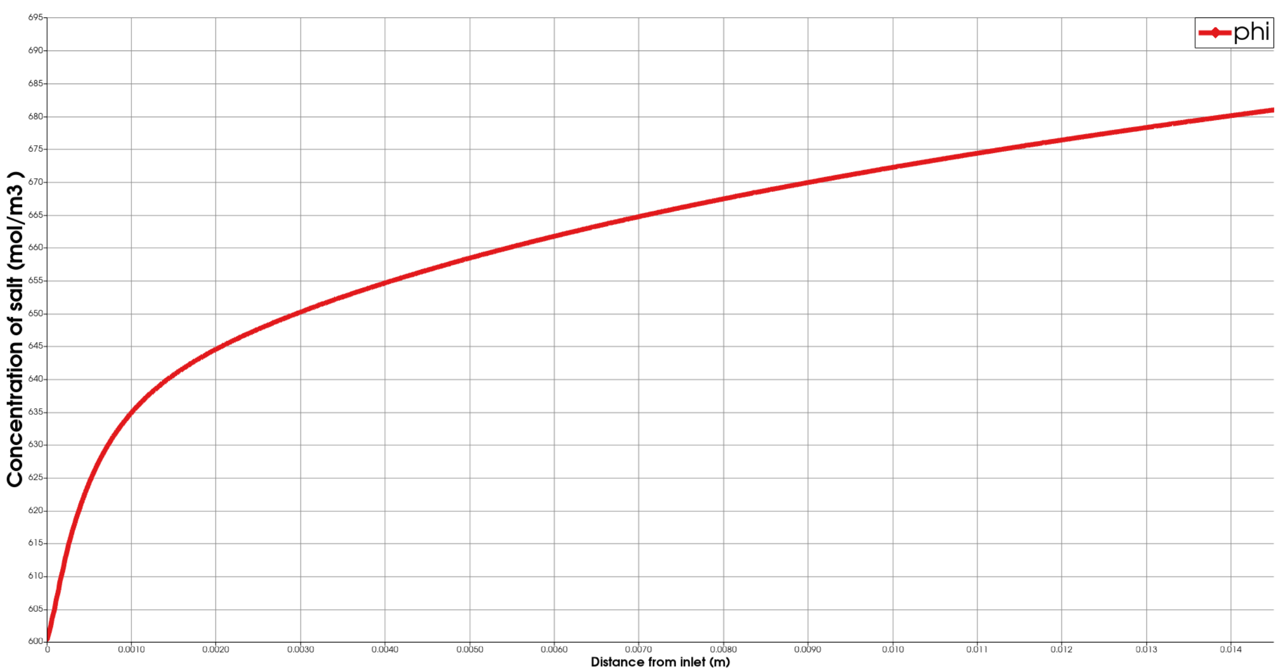

Figure 6.6: Concentration profile at the membrane. Simulation conditions: $u_{in} = 0.1 m/s$, $\Delta P = \Delta P1$.

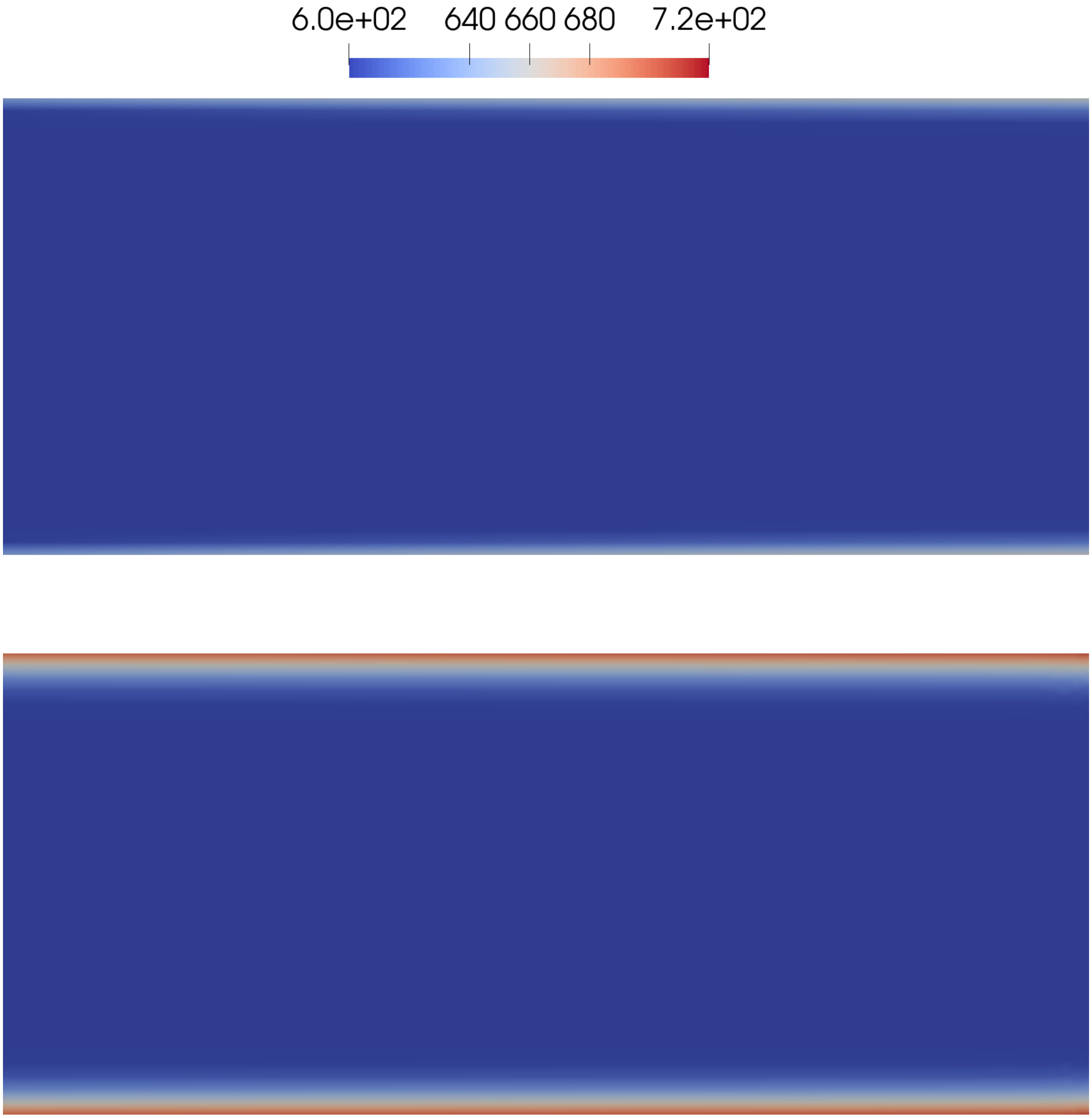

Figure 6.7: Zoom on the concentration field for a single channel. Simulation conditions: $u_{\text{in}} = 0.1m/s$, $\Delta P = \Delta P1$.

CHAPTER 7

Conclusions and future work

7.1 Conclusions.

In this thesis, a numerical method based on the Hybridizable Discontinuous Galerkin (HDG) scheme was developed and analyzed to solve a coupled system of Navier-Stokes and advection-diffusion equations, which models the reverse osmosis process in desalination channels. The proposed formulation stands out for its conservative nature and its ability to significantly reduce the size of the overall linear system compared to non-hybrid methods, which is especially advantageous in applications with high-order approximations. The validity of the scheme was verified under certain assumptions on the smallness of the data. Well-posedness of the proposed HDG scheme was analyzed using the following procedure. First, introduce a fixed-point operator to decouple the nonlinear scheme and obtain separate schemes for the Navier-Stokes and advection-diffusion equations. Second, well-posedness of each of these schemes was analyzed. Finally, Brouwer and Banach fixed-point theorems were employed to prove the existence and uniqueness of solution of the coupled scheme, under certain assumptions on the data.

In addition, error estimates were derived, showing that the proposed scheme provides optimal orders of convergence. Finally, numerical simulations were presented that demonstrated the good performance of the method compared to manufactured solutions and in realistic desalination scenarios.

7.2 Future work.

This work leaves several interesting possibilities for further exploration. One of them is to relax one of the assumptions in the well-posedness analysis. In particular, the assumption $c_1 h_e^{-1}$ bounded, even though c_1 is very small in reverse osmosis applications, it does not hold when h goes to zero. We believe that it is possible to relax this restriction and obtain valid results in more general contexts. It would also be interesting to extend the model to the time-dependent case. Incorporating temporal evolution would allow for a more realistic analysis of the dynamic behavior of the system, especially in non-stationary desalination processes.

Finally, a natural step would be to perform *a posteriori* error analysis. This would help to automatically identify areas where the method needs higher resolution, in particular near the membrane, which is useful for optimizing the use of computational resources and improving the accuracy of simulations.

Bibliography

[1] Isaac Bermudez, Victor Burgos, Jessika Camaño, Fernando Gajardo, Ricardo Oyarzúa, and Manuel Solano, *Mixed finite element methods for coupled fluid flow problems arising from reverse osmosis modeling*, Centro de Investigación en Ingeniería Matemática, serie de pre-publicaciones (2024).

[2] Isaac Bermúdez, Jessika Camaño, Ricardo Oyarzúa, and Manuel Solano, *A conforming mixed finite element method for a coupled Navier–Stokes/transport system modeling reverse osmosis processes*, Computer Methods in Applied Mechanics and Engineering **433** (2025), 117527.

[3] Nicolás Carro, David Mora, and Jesus Vellojin, *A finite element model for concentration polarization and osmotic effects in a membrane channel*, International Journal for Numerical Methods in Fluids **96** (2024), no. 5, 601–625.

[4] Aycil Cesmelioglu, Bernardo Cockburn, and Weifeng Qiu, *Analysis of a hybridizable discontinuous Galerkin method for the steady-state incompressible Navier-Stokes equations*, Mathematics of Computation **86** (2016), no. 306, 1643–1670.

[5] Aycil Cesmelioglu and Sander Rhebergen, *A hybridizable discontinuous Galerkin method for the coupled Navier-stokes and Darcy problem*, Journal of Computational and Applied Mathematics **422** (2023), 114923.

[6] Aycil Cesmelioglu, Sander Rhebergen, and Garth N. Wells, *An embedded–hybridized discontinuous Galerkin method for the coupled Stokes–Darcy system*, Journal of Computational and Applied Mathematics **367** (2020), 112476.

[7] Daniele Antonio Di Pietro and Alexandre Ern, *Mathematical aspects of discontinuous Galerkin methods*, Springer Berlin Heidelberg, 2012.

[8] Joyner Eke, Ahmed Yusuf, Adewale Giwa, and Ahmed Sodiq, *The global status of desalination: An assessment of current desalination technologies, plants and capacity*, Desalination **495** (2020), 114633.

[9] Alexandre Ern and Jean-Luc Guermond, *Theory and practice of finite elements*, Springer New York, 2004.

[10] Guosheng Fu and Christoph Lehrenfeld, *A strongly conservative hybrid dg/mixed fem for the coupling of Stokes and Darcy flow*, Journal of Scientific Computing **77** (2018), no. 3, 1605–1620.

[11] Gabriel N. Gatica, *A simple introduction to the mixed finite element method: Theory and applications*, Springer International Publishing, 2014.

[12] Vivette Girault and Béatrice Rivière, *Dg approximation of coupled navier–stokes and darcy equations by beaver–joseph–saffman interface condition*, SIAM Journal on Numerical Analysis **47** (2009), no. 3, 2052–2089.

[13] Keegan L. A. Kirk and Sander Rhebergen, *Analysis of a pressure-robust hybridized discontinuous Galerkin method for the stationary Navier–Stokes equations*, Journal of Scientific Computing **81** (2019), no. 2, 881–897.

[14] Sander Rhebergen and Garth N. Wells, *Analysis of a hybridized/interface stabilized finite element method for the Stokes equations*, SIAM Journal on Numerical Analysis **55** (2017), no. 4, 1982–2003.

[15] Sander Rhebergen and Garth N. Wells, *Analysis of a hybridized/interface stabilized finite element method for the Stokes equations*, SIAM Journal on Numerical Analysis **55** (2017), no. 4, 1982–2003.

[16] Sander Rhebergen and Garth N. Wells, *A hybridizable discontinuous Galerkin method for the Navier–Stokes equations with pointwise divergence-free velocity field*, Journal of Scientific Computing **76** (2018), no. 3, 1484–1501.

[17] Sander Rhebergen and Garth N. Wells, *Preconditioning of a hybridized discontinuous Galerkin finite element method for the Stokes equations*, Journal of Scientific Computing **77** (2018), no. 3, 1936–1952.

[18] J Schöberl, *C++11 implementation of finite elements in ngsolve (asc report 30/2014; pp. 1–23).* ., Institute of Analysis and Scientific Computing, TU Wien (2014).

[19] Clara Skuse, Alejandro Gallego-Schmid, Adisa Azapagic, and Patricia Gorgojo, *Can emerging membrane-based desalination technologies replace reverse osmosis?*, Desalination **500** (2021), 114844.

[20] Arun Subramani, Suhan Kim, and Eric M.V. Hoek, *Pressure, flow, and concentration profiles in open and spacer-filled membrane channels*, Journal of Membrane Science **277** (2006), no. 1, 7–17.

[21] Garth N. Wells, *Analysis of an interface stabilized finite element method: The advection-diffusion-reaction equation*, SIAM Journal on Numerical Analysis **49** (2011), no. 1, 87–109.